Total Ionizing Dose Test Report

No. 13T-RTAX4000D-CQ352-D6NR61

July 16, 2013

Table of Contents

TOTAL IONIZING DOSE TEST REPORT

13T-RTAX4000D-CQ352-D6NR61

July 16, 2013

CK Huang and J.J. Wang

(408) 643-6136, 643-6302

chang-kai.huang@microsemi.com, jih-jong.wang@microsemi.com

I. Summary Table

The TID tolerance for each tested parameter is summarized below in Table 1. The overall tolerance is limited by the standby power-supply current (ICC). The room temperature annealing allowed by 1019.8 to anneal down ICC is performed for approximately 7 days. Every DUT passes the major specifications listed in the table for 200 krad (SiO2) of irradiation.

Table 1 Tolerances for Each Tested Parameter

Parameter	Tolerance
1. Gross Functionality	Passed 300 krad (SiO_2)
2. Power Supply Current (ICCA/ICCI)	Passed 200 krad (SiO_2)
3. Input Threshold (VIL/VIH)	Passed 300 krad (SiO_2)
4. Output Drive (VOL/VOH)	Passed 300 krad (SiO_2)
5. Propagation Delay	Passed 300 krad (SiO_2) for 10% degradation criterion
6. Transition Time	Passed 300 krad (SiO_2)

II. Total Ionizing Dose (TID) Testing

This testing is designed on the basis of an extensive database (see, for example, TID data of antifuse-based FPGAs at http://www.klabs.org and http://www.microsemi.com/soc) accumulated from the TID testing of many generations of antifuse-based FPGAs.

A. Device-Under-Test (DUT) and Irradiation Parameters

Table 2 lists the DUT and irradiation parameters. During irradiation all inputs are grounded except for the inputs Burnin, oe_EAQ, enable_HSB and the utilized clocks (Rclock1-3 and Hclock1-4). The inputs Burnin, oe_EAQ and enable_HSB are set high to 3.3 V and a 1 KHz clock is provided to all clocks in order for the design to remain stable during irradiation. During anneal each input and output is tied to ground or VCCI through a 4.7 kΩ resistor. Appendix A contains the schematics of irradiation-bias circuits.

Table 2 DUT and Irradiation Parameters

Part Number	RTAX4000D
Package	CQFP352
Foundry	United Microelectronics Corp.
Technology	0.15 µm CMOS
DUT Design	RTAX4000D_CQ352_MASTER
Die Lot Number	D6NR61
Quantity Tested	6
Serial Number	300 krad: 3401, 3402, 3411 200 krad: 3413, 3421, 3429
Radiation Facility	Defense Microelectronics Activity
Radiation Source	Co-60
Dose Rate (±5%)	10 krad (SiO_2)/min
Irradiation Temperature	Room
Irradiation and Measurement Bias (VCCI/VCCA)	Static at 3.3 V / 1.5 V
I/O Configuration	Single ended: LVTTL Differential pair: LVPECL

B. Test Method

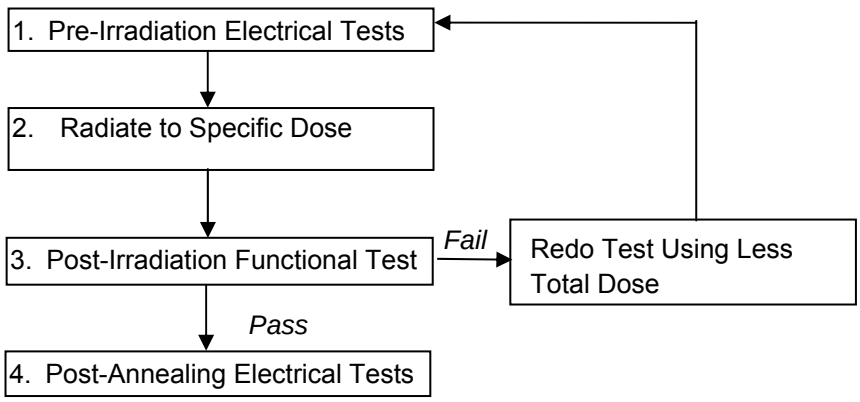

Figure 1 Parametric Test Flow Chart

The test method generally follows the guidelines in the military standard TM1019.8. Figure 1 is the flow chart showing the steps for parametric tests, irradiation, and post-irradiation annealing.

The accelerated aging, or rebound test mentioned in TM1019.8, is unnecessary because there is no adverse time-dependent effect (TDE) in Microsemi SoC Products Group products manufactured by sub-micron CMOS technology. Elevated temperature annealing actually reduces the effects originated from radiation-induced leakages. As indicated by testing data in the following sections, the predominant radiation effects in RTAX4000D are due to radiation-induced leakages.

Room temperature annealing is performed in this test; the duration is approximately 7 days.

C. Design and Parametric Measurements

The DUT uses a high utilization generic design (RTAX4000D_CQ352_MASTER) to evaluate total dose effects for typical space applications. The schematics of this design are documented in Appendix B.

The functionality is measured at 1 MHz and 50 MHz using the minimum and maximum power specifications shown in Table 3.

Table 3 Minimum and Maximum Power Specifications for RTAX-D Devices

Supply Voltage	Minimum	Recommended	Maximum
1.5 V Core	1.4 V	1.5 V	1.6 V
3.3 V I/O	3.0 V	3.3 V	3.6 V
3.3 V VCCDA I/O	3.0 V	3.3 V	3.6 V

The functionality test design is subdivided into two blocks, the EAQ (Enhanced Antifuse Qualification) and the QBI (Qualification Burn-In). The EAQ block includes three 1458-bit shift registers and tests the I/Os (1560 I/O registers and 520 I/Os) and RAM (1x16384 RAM). The QBI block tests all offered macros and I/O standards. The results from the functional tests are obtained from the following outputs: IO_Monitor_EAQ, RAM_Monitor_EAQ, Array_Monitor_EAQ, Global_Monitor_EAQ, C_test_mon_QBI, ALU_test_mon_QBI, Global_mon_QBI_TP, and Global_mon_QBI_BI. Details on the Functionality Test are shown in Appendix B.

ICC is measured on the power supply of the logic-array (ICCA) and I/O (ICCI) respectively. The input logic threshold (VIL/VIH) is tested on single-ended inputs Shiftin1, Shiftin2, Shiftin3, Shiftin4, Shiftin5, Shiftin7, Shiftin8, zoom_sel_n_1, zoom_sel_n_0, zoom, TOG_n, SEU_sel, Set_n, Resetn, oe_EAQ, enable_HSB, test_done_sel_2, IO_Pattern_Length_2, IO_Pattern_Length_1, IO_Pattern_Length_0, IO_Johnson, A_Johnson, A_Pattern_Length_1, and A_Pattern_Length_0. The output-drive voltage (VOL/VOH) is measured on single-ended outputs Array_out_EAQ_0, Array_out_EAQ_1, Array_out_EAQ_2, Global_Monitor_EAQ, Shiftout3, Shiftout7, Shiftout8, RAM_Monitor_EAQ, RAM_out_EAQ_0, RAM_out_EAQ_4, RAM_out_EAQ_8.

The propagation delays are measured on the outputs of five delay strings; each one comprises of 1,170 NAND4-inverters. There are 6 delay measurements: one measurement for each delay string and a total delay measurement obtained from cascading all the delay strings. The propagation delay is defined as the time delay from the triggering edge at the HClock1 input to the switching edge at the output. The transition characteristics, measured on the output delay_out_SEU4, are shown as oscilloscope captures.

Table 4 lists measured electrical parameters and the corresponding logic design.

Table 4 Logic Design for Parametric Measurements

Parameters	Logic Design
1. Functionality	IO_Monitor_EAQ, RAM_Monitor_EAQ, Array_Monitor_EAQ, Global_Monitor_EAQ, C_test_mon_QBI, ALU_test_mon_QBI, Global_mon_QBI_TP, and Global_mon_QBI_BI
2. ICC (ICCA/ICCI)	DUT power supply
3. Input Threshold (VIL/VIH)	Single ended inputs (Shiftin1, Shiftin2, Shiftin3, Shiftin4, Shiftin5, Shiftin7, Shiftin8, zoom_sel_n_1, zoom_sel_n_0, zoom, TOG_n, SEU_sel, Set_n, Resetn, oe_EAQ, enable_HSB, test_done_sel_2, IO_Pattern_Length_2, IO_Pattern_Length_1, IO_Pattern_Length_0, IO_Johnson, A_Johnson, A_Pattern_Length_1, A_Pattern_Length_0)
4. Output Drive (VOL/VOH)	Single-ended outputs (Array_out_EAQ_0, Array_out_EAQ_1, Array_out_EAQ_2, Global_Monitor_EAQ, Shiftout3, Shiftout7, Shiftout8, RAM_Monitor_EAQ, RAM_out_EAQ_0, RAM_out_EAQ_4, RAM_out_EAQ_8)
5. Propagation Delay	String of NAND4-inverters. Measured from output delay_out_SEU4
6. Transition Characteristic	NAND4-inverter output (delay_out_SEU4)

III. Test Results

The test results mainly compare the electrical parameter measured pre-irradiation with the same parameter measured post-irradiation-and-annealing, or post-annealing.

A. Functionality

Every DUT passed the pre-irradiation and post-annealing functional tests.

B. Power Supply Current (ICCA and ICCI)

The logic-array power supply (VCCA) is 1.5 V, and the IO power supply (VCCI) is 3.3 V. Their standby currents, ICCA and ICCI, are monitored influx. Figure 2-7 show the influx ICCA and ICCI versus total dose for the DUTs.

Referring to TM1019.8 subsection 3.11.2.c, the post-irradiation-parametric limit (PIPL) for the post-annealing ICC, should be defined as the addition of highest ICCI, ICCDA, and ICCDIFFA values in Table 2-6 of the *RTAX-S/SL and RTAX-DSP Radiation-Tolerant FPGAs datasheet* posted on the Microsemi SoC Products Group website:

http://www.microsemi.com/soc/documents/RTAXS_DS.pdf

Therefore, the PIPL for ICCA is 600 mA, and the PIPL for ICCI is 60 mA.

Table 5 summarizes the pre-irradiation, post-irradiation right after irradiation and before anneal, and post-annealing ICCA and ICCI data.

Table 5 Pre-irradiation, Post Irradiation and Post-Annealing ICC

DUT	Total Dose	ICCA (mA)			ICCI (mA)		
		Pre-Irrad.	Post-Irrad.	Post-Ann.	Pre-Irrad.	Post-Irrad.	Post-Ann.
3401	300 krad	10	150	16	13	274	93
3402	300 krad	11	170	16	13	245	82
3411	300 krad	10	177	13	13	248	81
3413	200 krad	9	19	6	13	89	58
3421	200 krad	9	15	8	13	87	55
3429	200 krad	11	13	9	13	71	53

Based on these PIPL, the post-annealing DUT passes both the ICCA and ICCI specification for 200 krad(SiO_2).

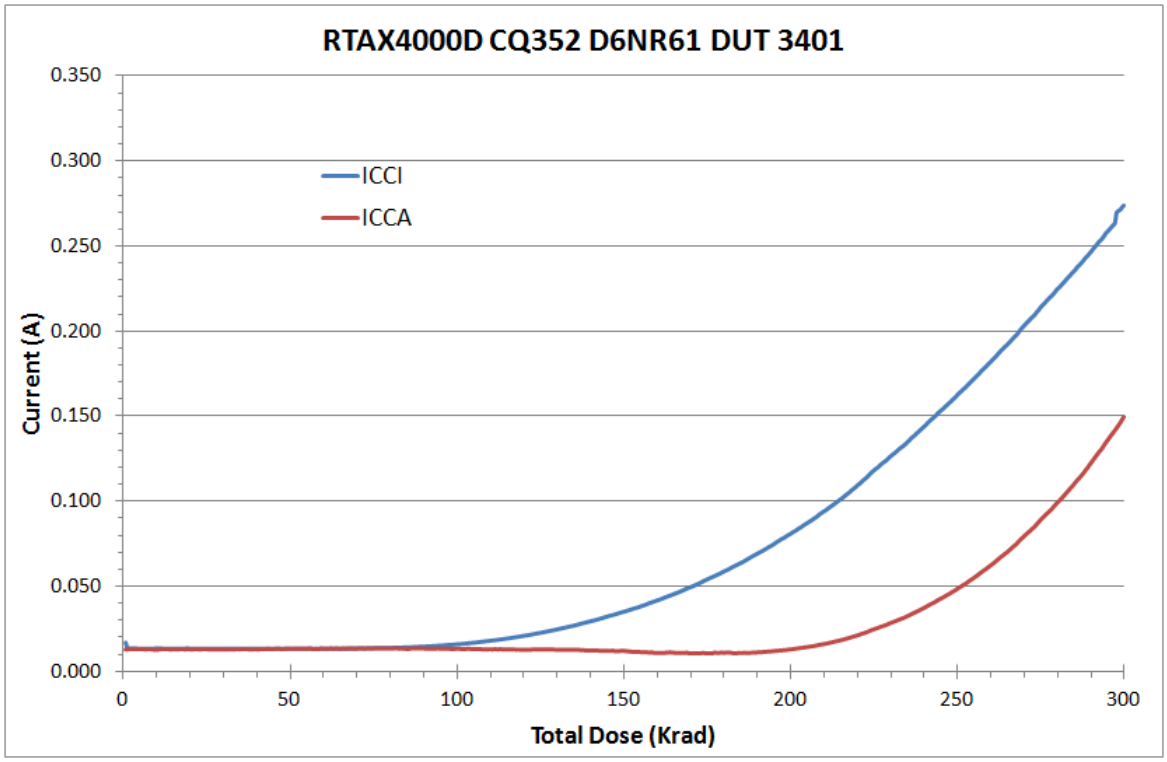

Figure 2 DUT 3401 Influx ICCI and ICCA

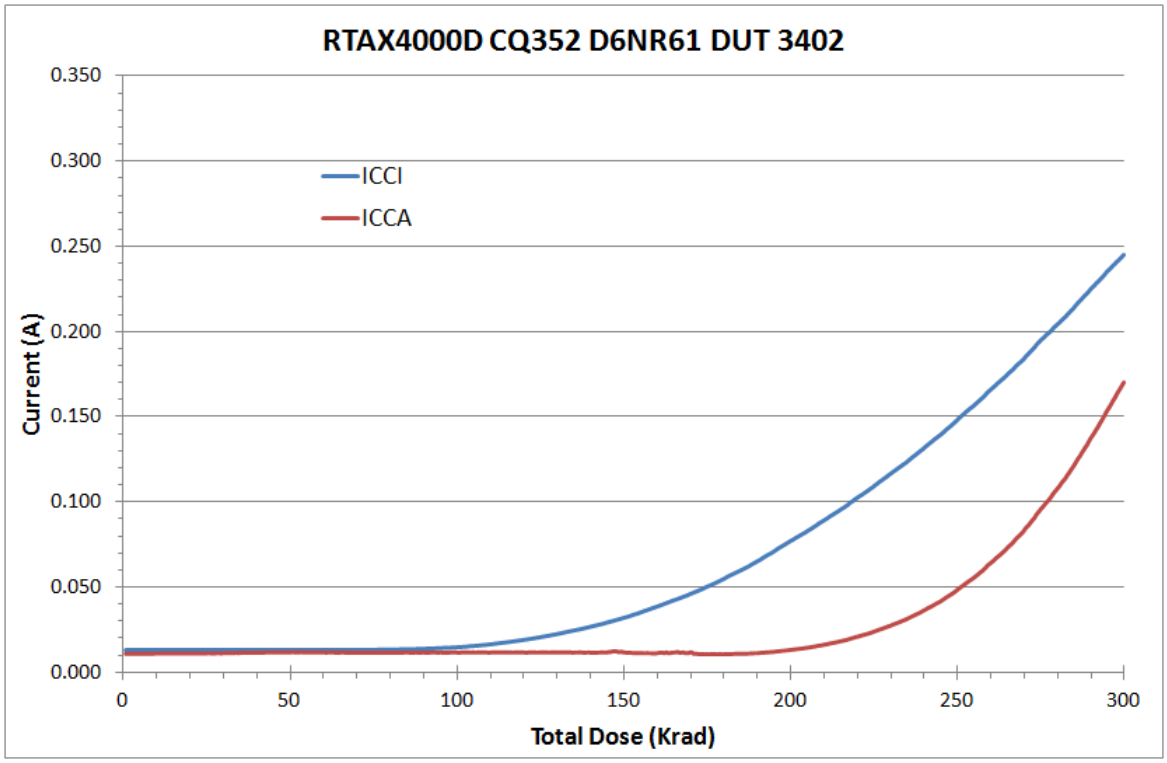

Figure 3 DUT 3402 Influx ICCI and ICCA

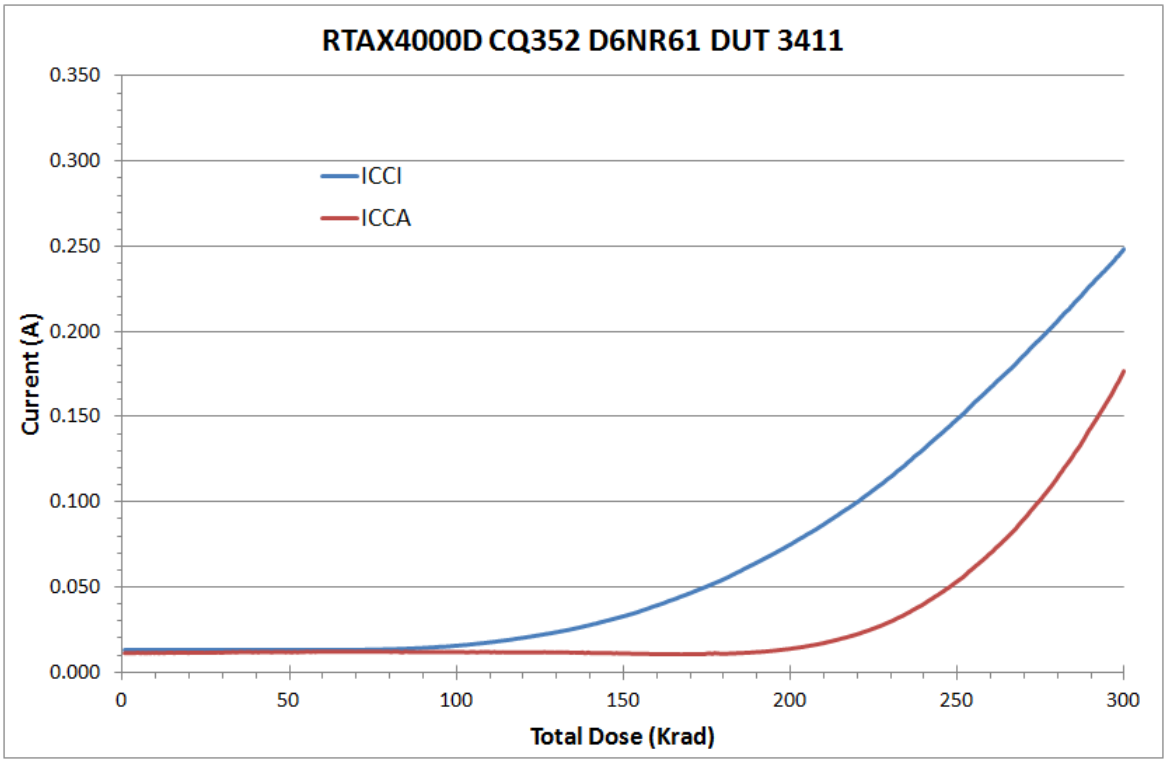

Figure 4 DUT 3411 Influx ICCI and ICCA

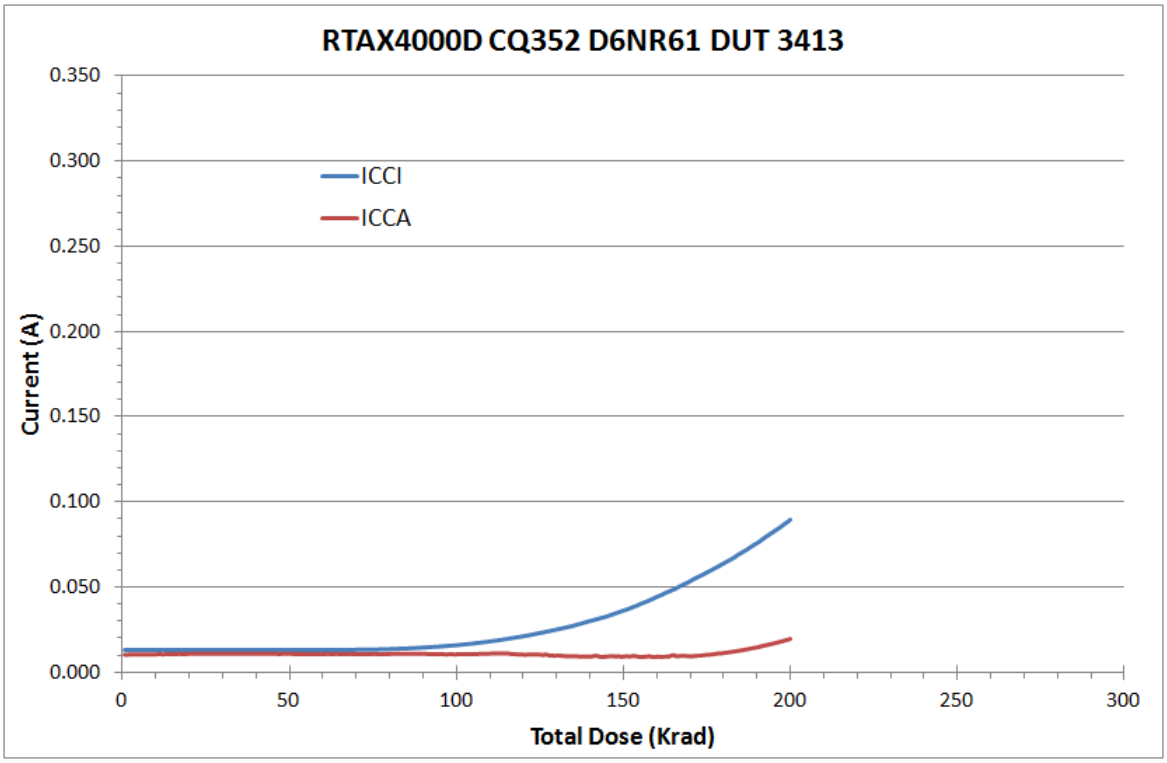

Figure 5 DUT 3413 Influx ICCI and ICCA

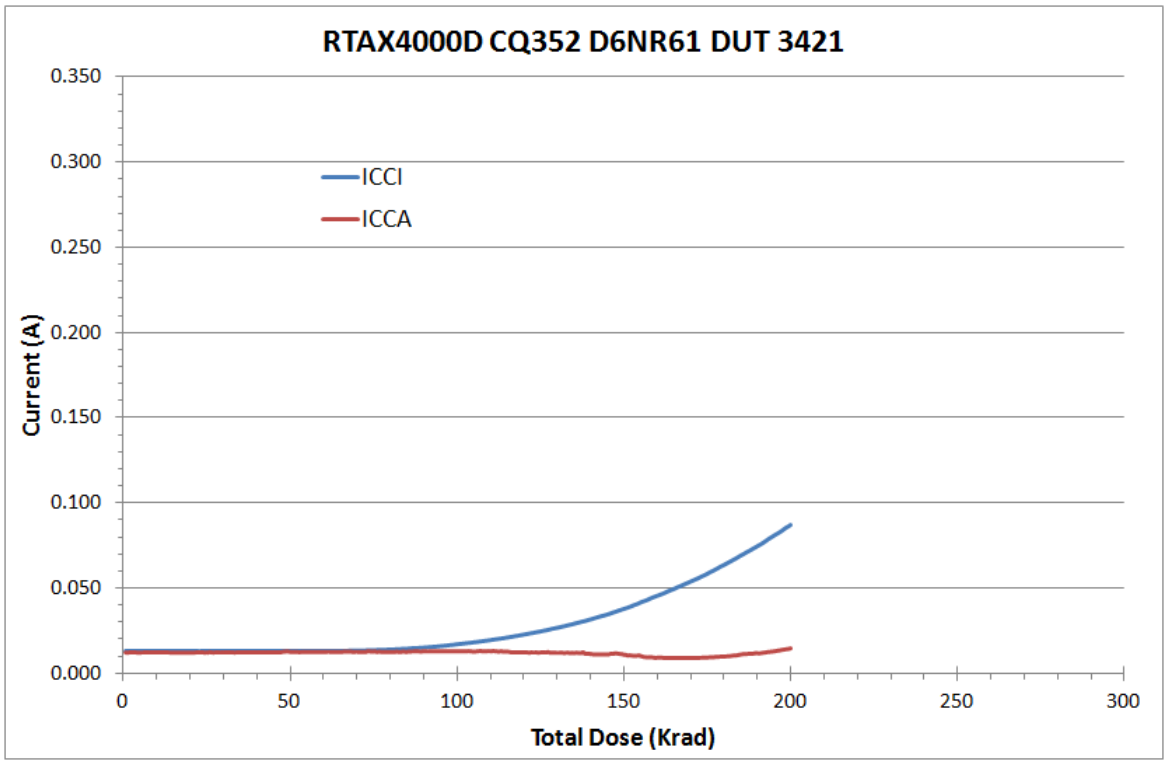

Figure 6 DUT 3421 Influx ICCI and ICCA

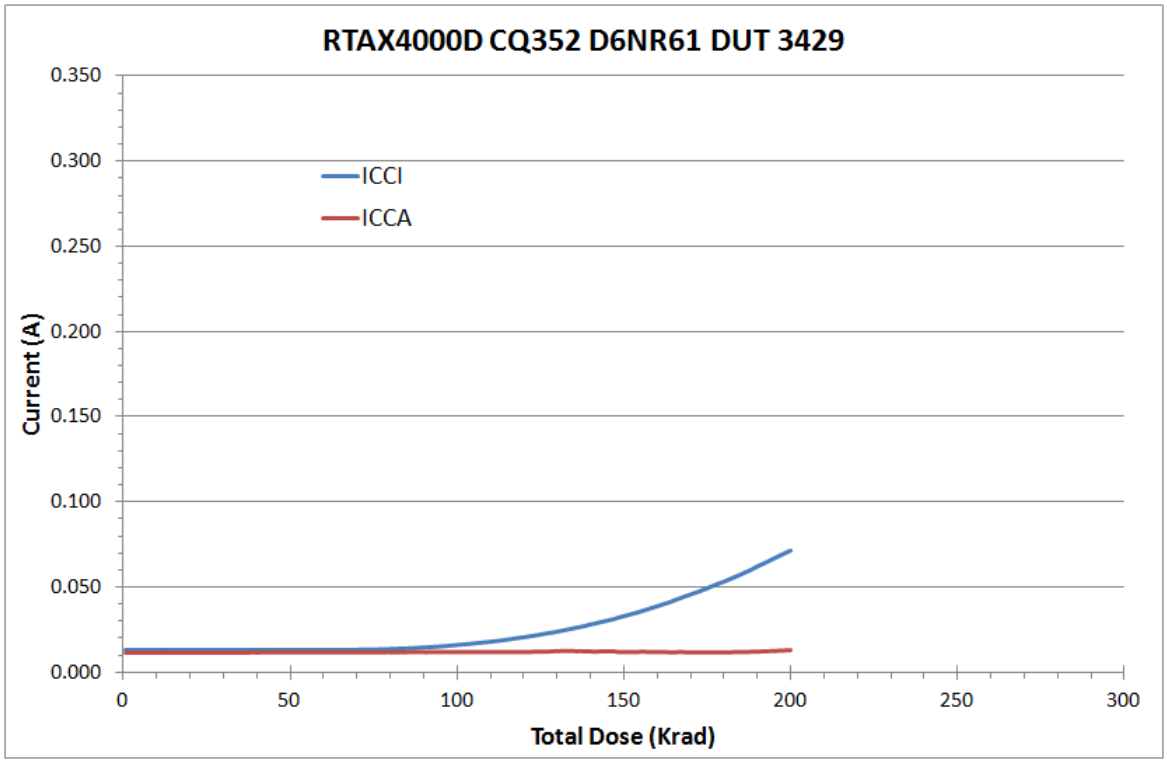

Figure 7 DUT 3429 Influx ICCI and ICCA

C. Single-Ended 3.3 V LVTTL Input Logic Threshold (VIL/VIH)

The input switching threshold, or trip point, is defined as the applied input voltage at which the output of the design, often just input and output buffers, starts to switch: VIH is the input trip point when the input is going high to low; VIL is the input trip point when the input is going low to high. They are listed in Tables 6 and 7. The difference between the pre-irradiation and post-annealing data is usually negligibly small.

Table 6 Pre-Irradiation and Post-Annealing VIL (V)

Pin \ DUT(Dose)	3401 (300 krad)		3402 (300 krad)		3411 (300 krad)		3413 (200 krad)		3421 (200 krad)		3429 (200 krad)	
	Pre-rad	Pos-an	Pre-rad	Pos-an	Pre-rad	Pos-an	Pre-rad	Pos-an	Pre-rad	Pos-an	Pre-rad	Pos-an
SEU_sel	1.36	1.34	1.36	1.34	1.36	1.34	1.36	1.35	1.36	1.34	1.37	1.35
zoom_sel_n_0	1.37	1.35	1.36	1.34	1.37	1.34	1.37	1.36	1.36	1.35	1.38	1.36
zoom_sel_n_1	1.36	1.34	1.36	1.34	1.36	1.34	1.37	1.35	1.36	1.34	1.37	1.35
zoom	1.36	1.35	1.35	1.34	1.36	1.35	1.36	1.36	1.35	1.35	1.37	1.36
TOG_n	1.37	1.37	1.37	1.37	1.37	1.37	1.38	1.37	1.37	1.37	1.37	1.37
Set_n	1.36	1.35	1.36	1.35	1.36	1.35	1.36	1.35	1.36	1.35	1.37	1.36
Resetn	1.36	1.36	1.36	1.35	1.36	1.36	1.37	1.36	1.37	1.36	1.37	1.37
oe_EAQ	1.37	1.35	1.38	1.36	1.38	1.36	1.38	1.36	1.37	1.36	1.37	1.36
enable_HSB	1.37	1.35	1.37	1.35	1.37	1.34	1.37	1.35	1.36	1.34	1.36	1.35
IO_Pattern_Length_1	1.37	1.37	1.37	1.36	1.37	1.37	1.38	1.37	1.37	1.36	1.37	1.37
IO_Pattern_Length_2	1.37	1.37	1.37	1.36	1.37	1.36	1.38	1.37	1.37	1.36	1.37	1.37

Table 7 Pre-Irradiation and Post-Annealing VIH (V)

Pin \ DUT(Dose)	3401 (300 krad)		3402 (300 krad)		3411 (300 krad)		3413 (200 krad)		3421 (200 krad)		3429 (200 krad)	
	Pre-rad	Pos-an	Pre-rad	Pos-an	Pre-rad	Pos-an	Pre-rad	Pos-an	Pre-rad	Pos-an	Pre-rad	Pos-an
SEU_sel	1.65	1.62	1.65	1.62	1.65	1.62	1.65	1.63	1.65	1.63	1.66	1.64
zoom_sel_n_0	1.64	1.62	1.64	1.61	1.64	1.61	1.65	1.63	1.64	1.62	1.65	1.63
zoom_sel_n_1	1.65	1.63	1.65	1.62	1.65	1.62	1.66	1.64	1.65	1.63	1.66	1.64
zoom	1.65	1.63	1.64	1.63	1.65	1.63	1.66	1.64	1.65	1.63	1.66	1.65
TOG_n	1.66	1.65	1.66	1.66	1.66	1.65	1.67	1.66	1.66	1.65	1.66	1.65
Set_n	1.65	1.64	1.65	1.64	1.65	1.64	1.65	1.64	1.64	1.63	1.66	1.65
Resetn	1.64	1.63	1.64	1.63	1.64	1.63	1.65	1.64	1.65	1.64	1.65	1.64
oe_EAQ	1.65	1.62	1.65	1.63	1.65	1.63	1.65	1.63	1.65	1.63	1.65	1.63
enable_HSB	1.66	1.63	1.65	1.63	1.65	1.63	1.66	1.64	1.65	1.63	1.65	1.63
IO_Pattern_Length_1	1.67	1.66	1.66	1.65	1.66	1.65	1.67	1.66	1.66	1.65	1.67	1.66
IO_Pattern_Length_2	1.65	1.64	1.65	1.63	1.65	1.64	1.66	1.65	1.64	1.63	1.65	1.64

D. Output-Drive Voltage (VOL/VOH)

The pre-irradiation and post-annealing VOL/VOH are listed in Tables 6 and 7. The post-annealing data are within the specification limits; in each case, the radiation-induced degradation is small.

Table 8 Pre-Irradiation and Post-Annealing VOL (mV)

Pin \ DUT(Dose)	3401 (300 krad)		3402 (300 krad)		3411 (300 krad)		3413 (200 krad)		3421 (200 krad)		3429 (200 krad)	
	Pre-rad	Pos-an	Pre-rad	Pos-an	Pre-rad	Pos-an	Pre-rad	Pos-an	Pre-rad	Pos-an	Pre-rad	Pos-an
Shiftout_0	190.8	182.2	188.2	179.4	192.4	183.7	193.3	185.0	190.1	181.8	188.1	180.4
Shiftout_5	179.7	171.2	181.5	173.0	180.5	171.8	182.2	173.6	182.2	174.2	180.4	172.5
Array_out_EAQ_0	169.8	161.3	170.2	161.0	170.6	161.4	172.0	163.8	171.1	163.0	169.4	161.6
Array_out_EAQ_2	179.4	171.1	182.5	173.8	180.3	171.2	180.8	172.6	181.4	174.0	181.4	173.7
delay_out_SEU_1	12.8	12.6	12.4	12.7	12.7	12.5	12.2	12.9	12.4	12.5	12.3	12.2
delay_out_SEU_4	13.3	13.1	12.8	13.2	13.3	13.6	13.3	13.3	13.1	12.8	13.0	13.0
RAM_Monitor_EAQ	17.4	16.7	17.4	16.8	17.4	16.9	17.2	16.8	17.2	16.7	17.4	16.5
RAM_out_EAQ_0	17.5	16.9	17.7	16.8	17.4	16.9	17.6	16.7	17.4	16.9	17.4	17.1
RAM_out_EAQ_4	17.1	16.2	17.3	16.4	16.9	16.6	16.9	16.4	16.8	16.6	17.1	16.3
RAM_out_EAQ_8	17.2	16.3	17.0	16.7	17.1	16.4	17.6	16.9	17.2	16.5	16.9	16.8

Table 9 Pre-Irradiation and Post-Annealing VOH (V)

Pin \ DUT(Dose)	3401 (300 krad)		3402 (300 krad)		3411 (300 krad)		3413 (200 krad)		3421 (200 krad)		3429 (200 krad)	
	Pre-rad	Pos-an	Pre-rad	Pos-an	Pre-rad	Pos-an	Pre-rad	Pos-an	Pre-rad	Pos-an	Pre-rad	Pos-an
Shiftout_0	2.72	2.71	2.72	2.72	2.72	2.71	2.72	2.71	2.72	2.72	2.72	2.72
Shiftout_5	2.73	2.73	2.73	2.73	2.73	2.73	2.73	2.73	2.73	2.73	2.73	2.73
Array_out_EAQ_0	2.74	2.74	2.74	2.74	2.74	2.74	2.74	2.74	2.74	2.74	2.75	2.74
Array_out_EAQ_2	2.73	2.73	2.73	2.72	2.73	2.73	2.73	2.73	2.73	2.73	2.73	2.73
delay_out_SEU_1	2.96	2.96	2.96	2.96	2.96	2.96	2.96	2.96	2.96	2.96	2.96	2.96
delay_out_SEU_4	2.96	2.96	2.96	2.96	2.96	2.96	2.96	2.96	2.96	2.96	2.96	2.96
RAM_Monitor_EAQ	2.96	2.96	2.96	2.96	2.96	2.96	2.96	2.96	2.96	2.96	2.96	2.96
RAM_out_EAQ_0	2.96	2.96	2.96	2.96	2.96	2.96	2.96	2.96	2.96	2.96	2.96	2.96
RAM_out_EAQ_4	2.96	2.96	2.96	2.96	2.96	2.96	2.96	2.96	2.96	2.96	2.96	2.96
RAM_out_EAQ_8	2.96	2.96	2.96	2.96	2.96	2.96	2.96	2.96	2.96	2.96	2.96	2.96

E. Propagation Delay

Table 8 lists the pre-irradiation and post-annealing propagation delays. The results show small radiation effects; in any case, the percentage change is well below 10%.

Table 10 Radiation-Induced Propagation Delay Degradations

Delay (µs)

DUT	Total Dose	Pre-rad.	Post-100krad	Post-200krad	Post-300krad	Post-ann.
3401	300 krad	7.200	7.146	7.144	7.255	7.400
3402	300 krad	7.219	7.165	7.152	7.248	7.340
3411	300 krad	7.158	7.110	7.099	7.203	7.265
3413	200 krad	7.295	7.261	7.256	-	7.345
3421	200 krad	7.268	7.211	7.207	-	7.375
3429	200 krad	7.060	7.007	6.995	-	7.145

Radiation Δ (%)

DUT	Total Dose	Pre-rad.	Post-100krad	Post-200krad	Post-300krad	Post-ann.
3401	300 krad	-	-0.7%	-0.8%	0.8%	2.8%
3402	300 krad	-	-0.8%	-0.9%	0.4%	1.7%
3411	300 krad	-	-0.7%	-0.8%	0.6%	1.5%
3413	200 krad	-	-0.5%	-0.5%	-	0.7%
3421	200 krad	-	-0.8%	-0.8%	-	1.5%
3429	200 krad	-	-0.7%	-0.9%	-	1.2%

F. Transition Time

Figure 8a to Figure 19b show the pre-irradiation and post-annealing transition edges. In each case, the radiation-induced transition-time degradation is not observable.

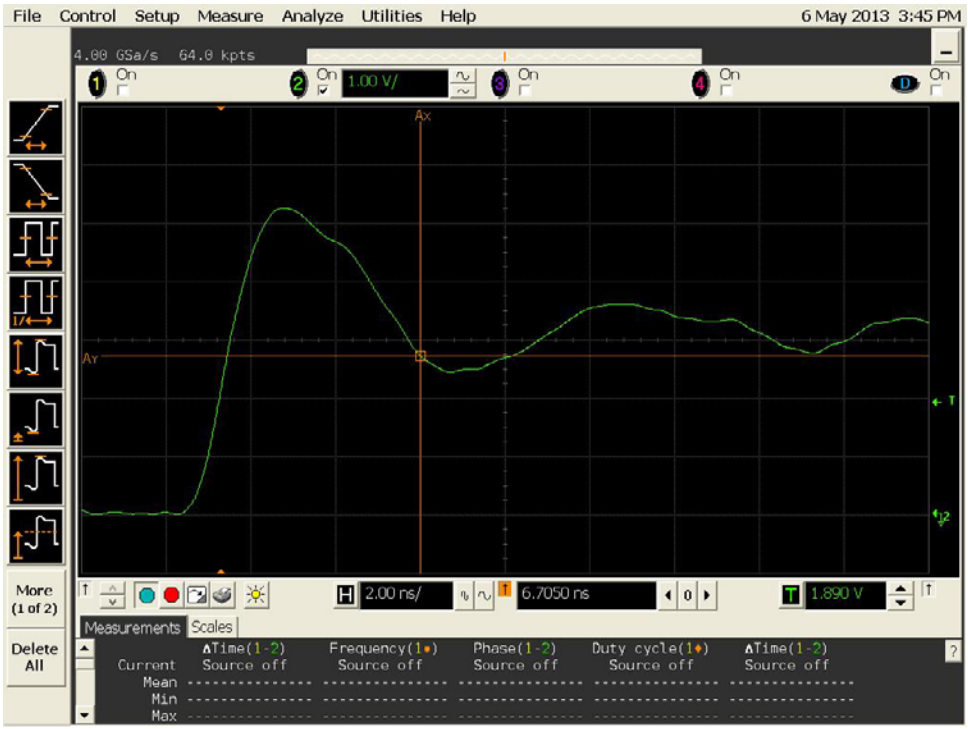

Figure 8a DUT 3401 Pre-Irradiation Rising Edge.

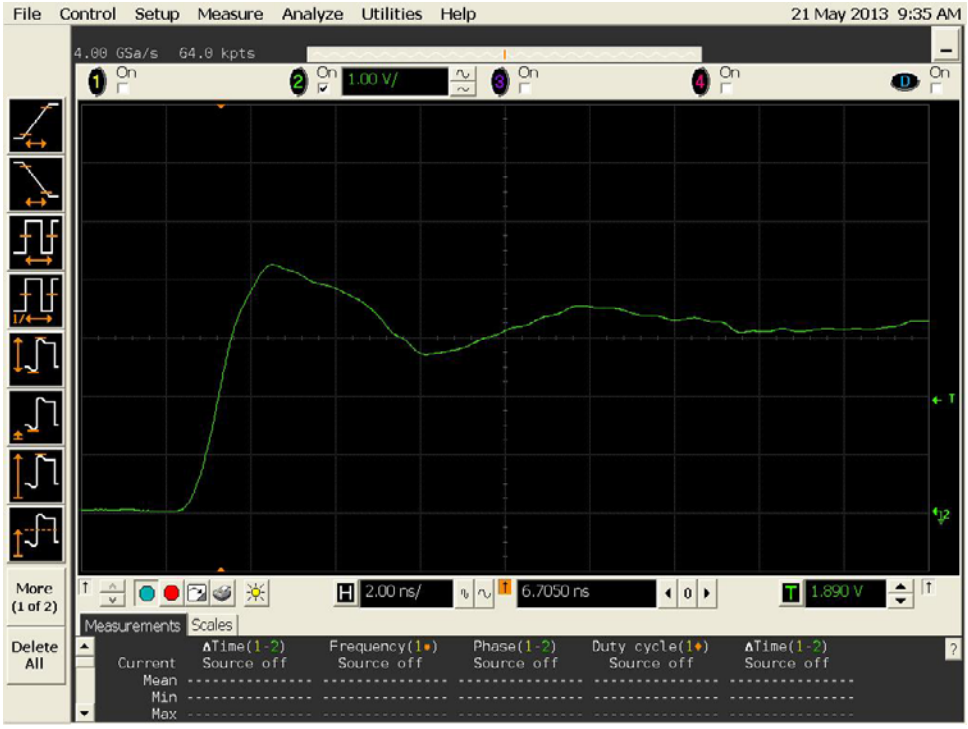

Figure 8b DUT 3401 Post-Annealing Rising Edge.

Figure 9a DUT 3402 Pre-irradiation Rising Edge.

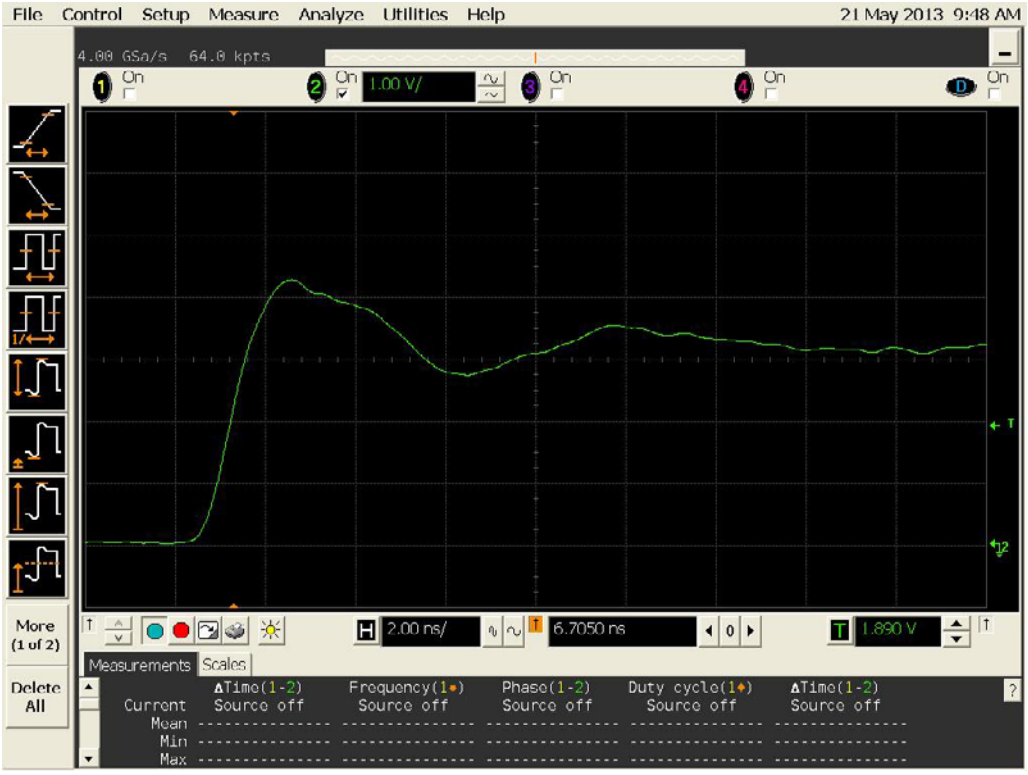

Figure 9b DUT 3402 Post-Annealing Rising Edge.

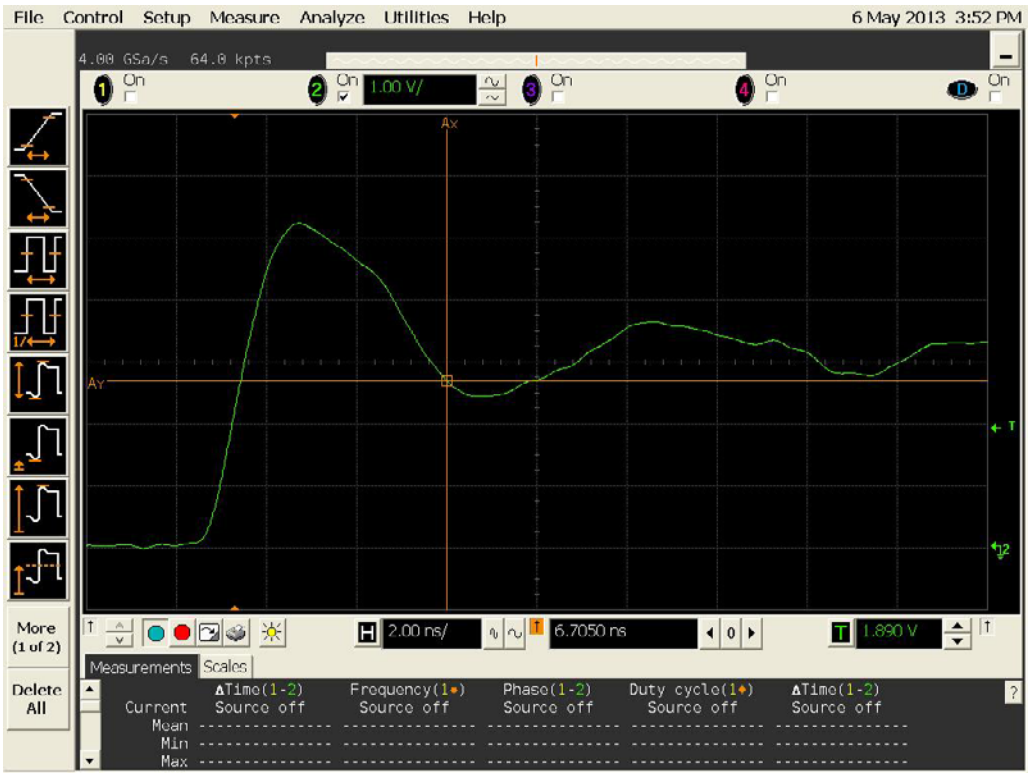

Figure 10a DUT 3411 Pre-Irradiation Rising Edge.

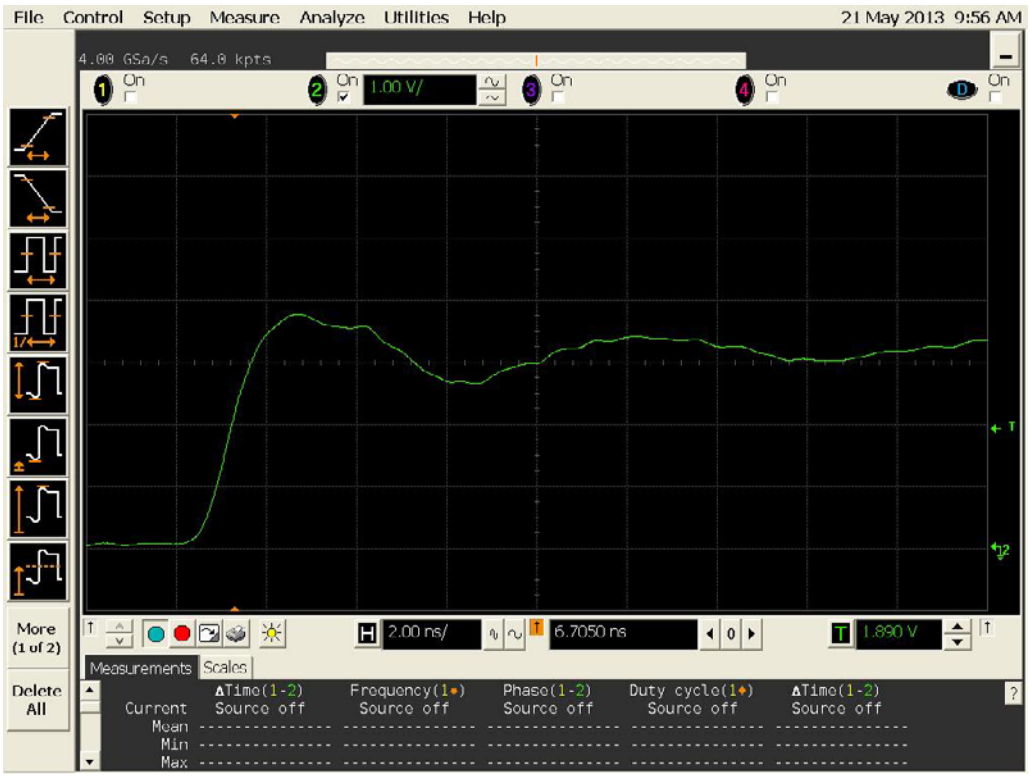

Figure 10b DUT 3411 Post-Annealing Rising Edge.

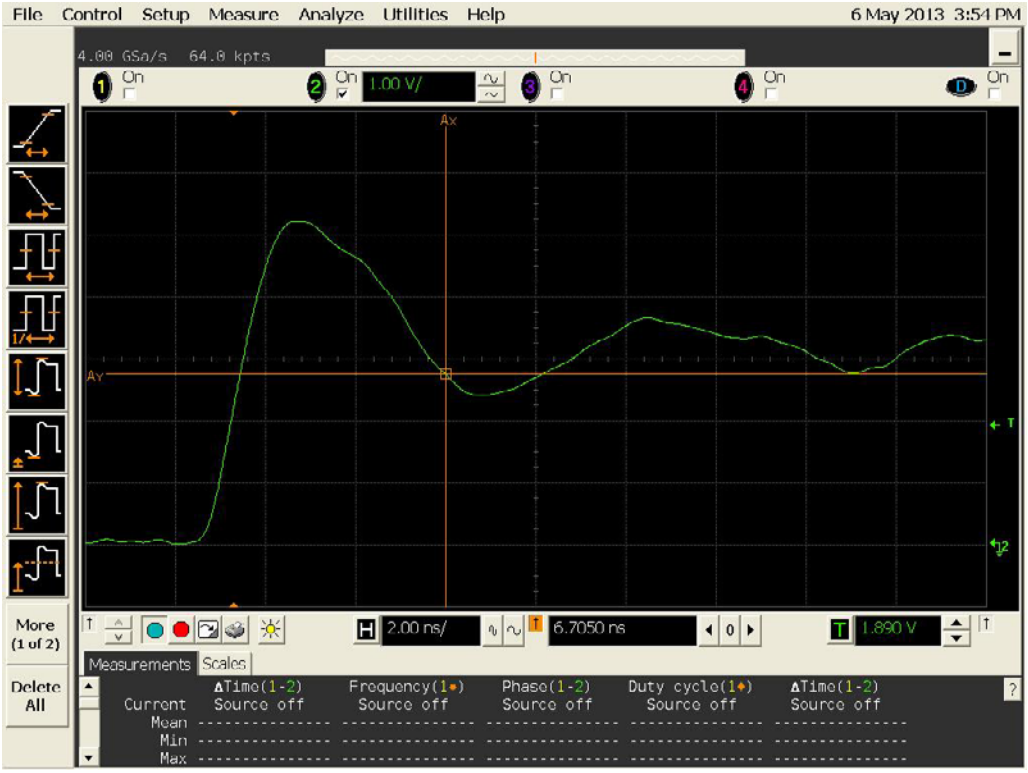

Figure 11a DUT 3413 Pre-Irradiation Rising Edge.

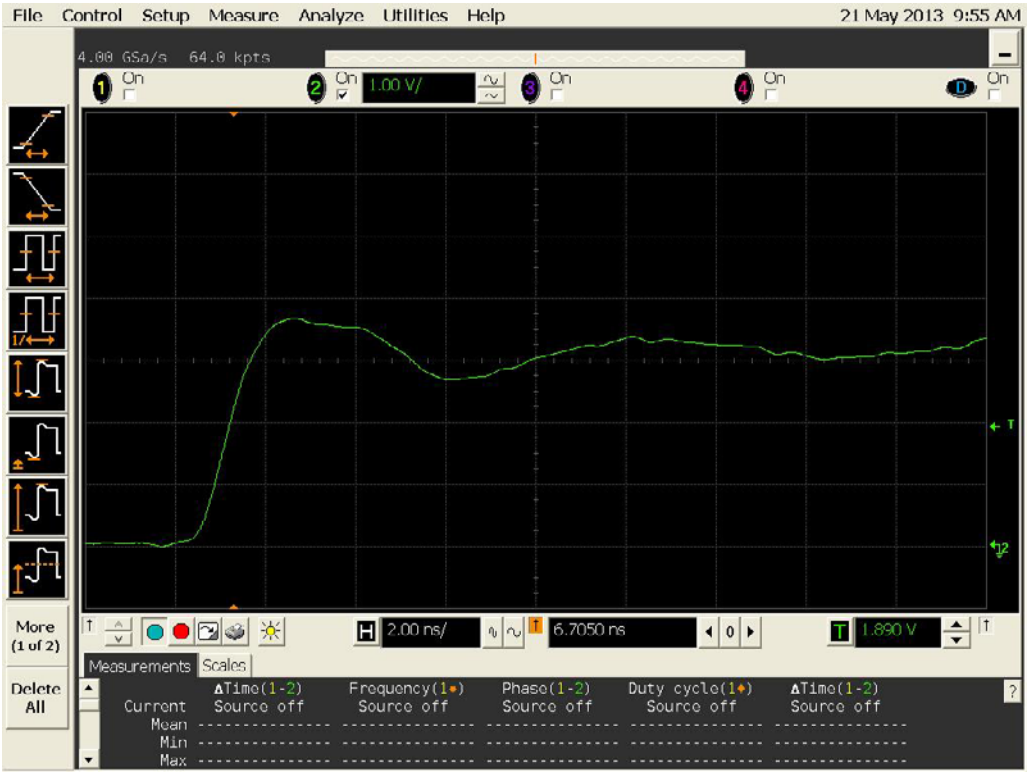

Figure 11b DUT 3413 Post-Annealing Rising Edge.

Figure 12a DUT 3421 Pre-Irradiation Rising Edge.

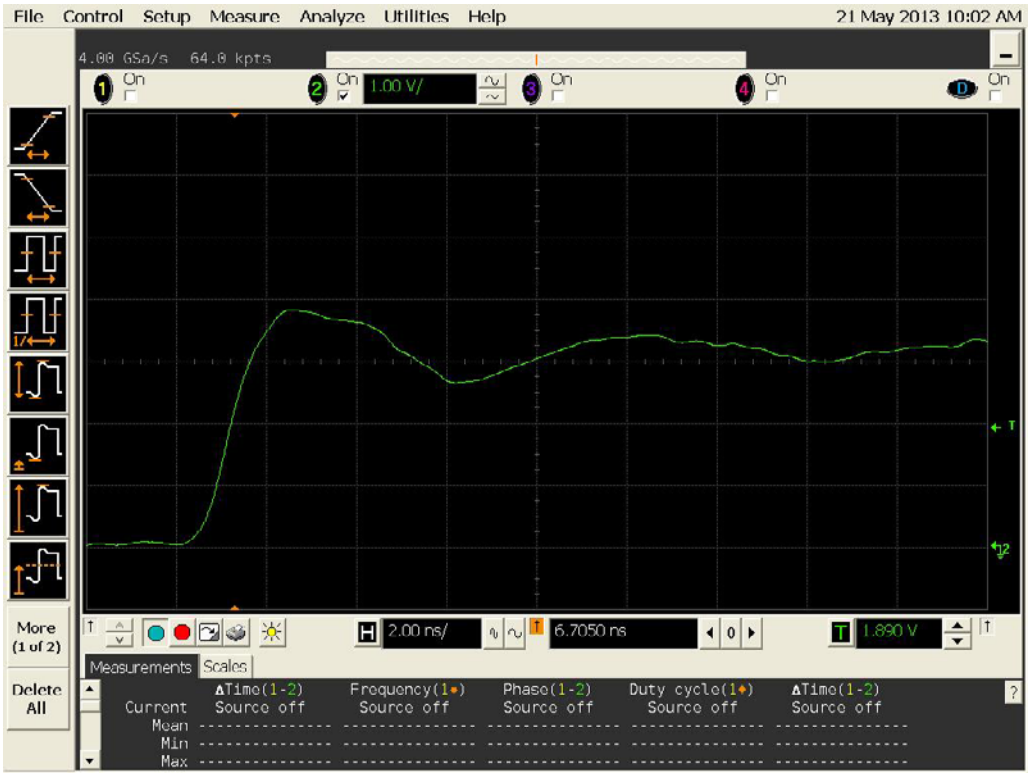

Figure 12b DUT 3421 Post-Annealing Rising Edge.

Figure 13a DUT 3429 Pre-Irradiation Rising Edge.

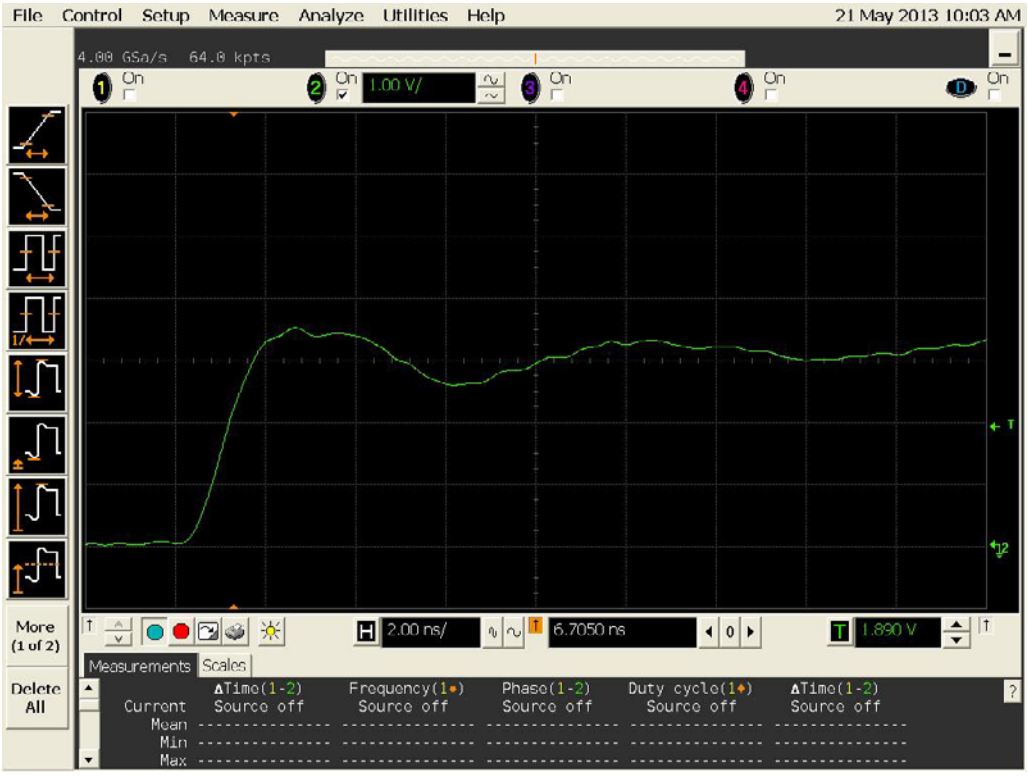

Figure 13b DUT 3429 Post-Annealing Rising Edge.

Figure 14a DUT 3401 Pre-Irradiation Falling Edge.

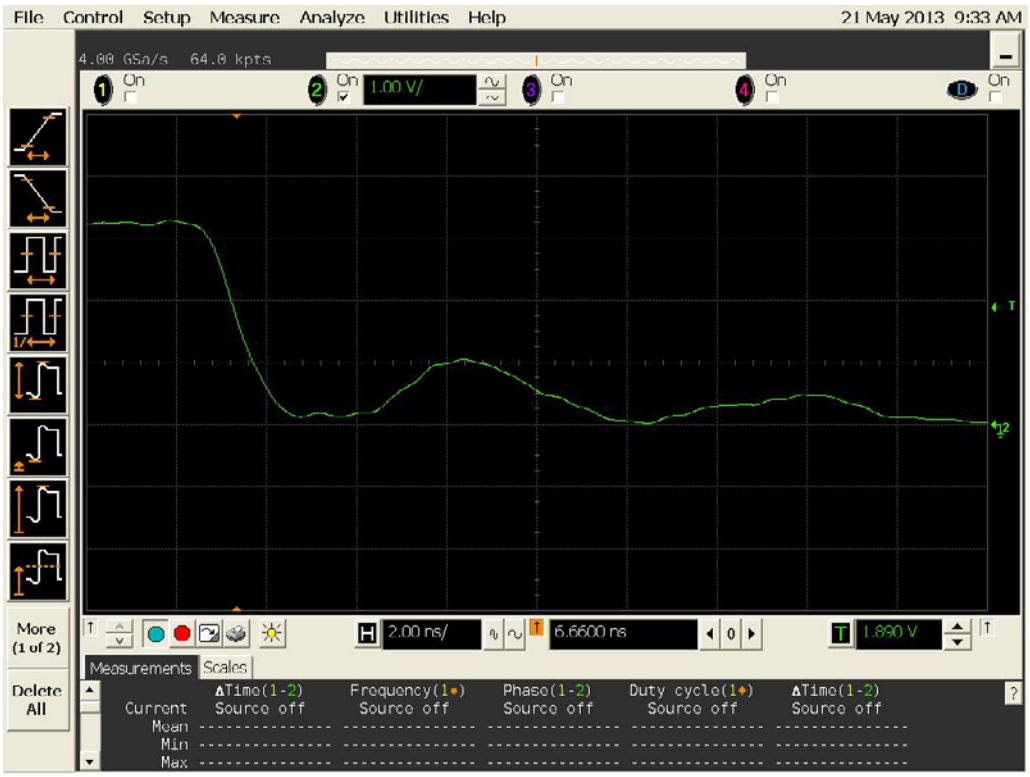

Figure 14b DUT 3401 Post-Annealing Falling Edge.

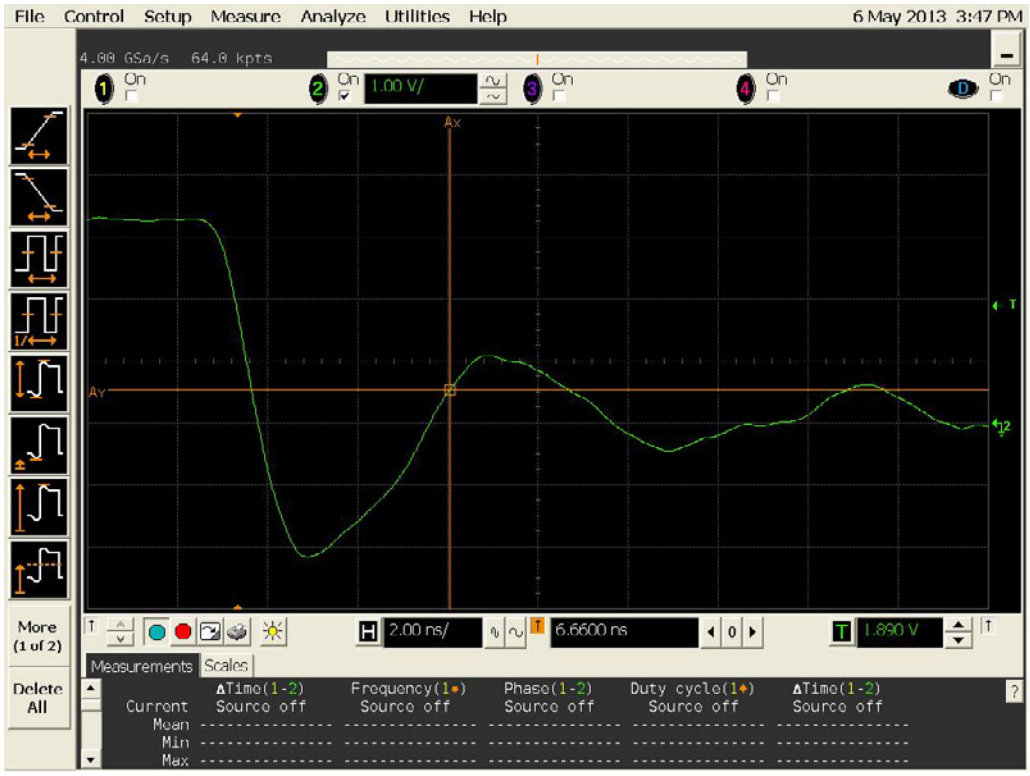

Figure 15a DUT 3402 Pre-Irradiation Falling Edge.

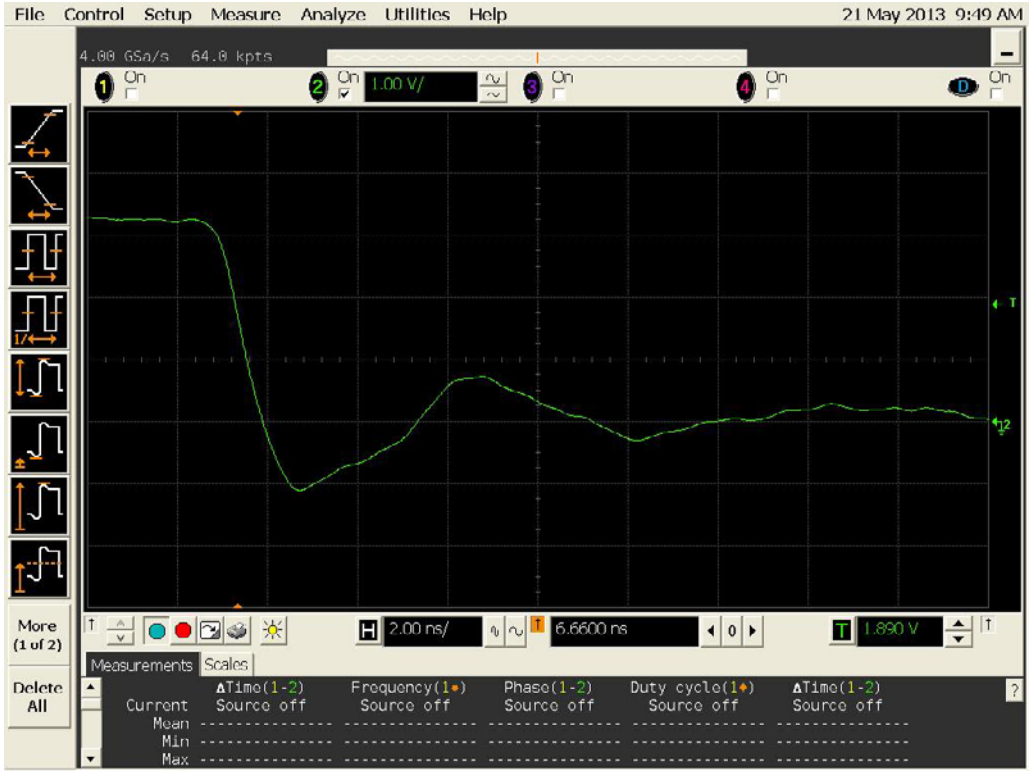

Figure 15b DUT 3402 Post-Annealing Falling Edge.

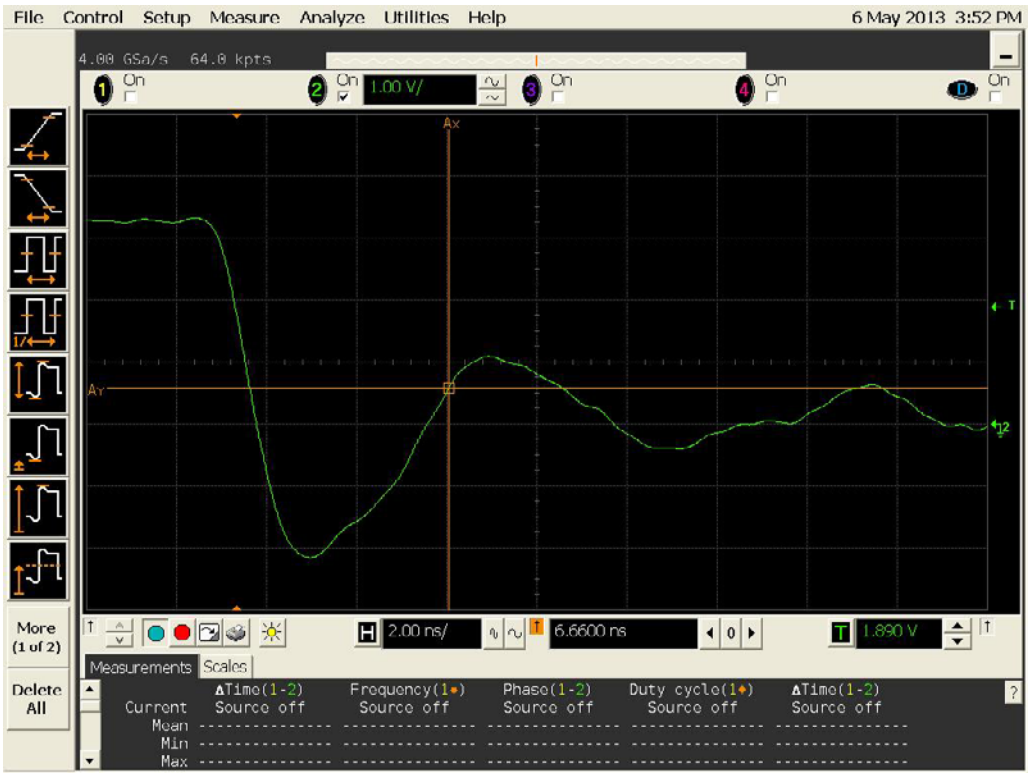

Figure 16a DUT 3411 Pre-Irradiation Falling Edge.

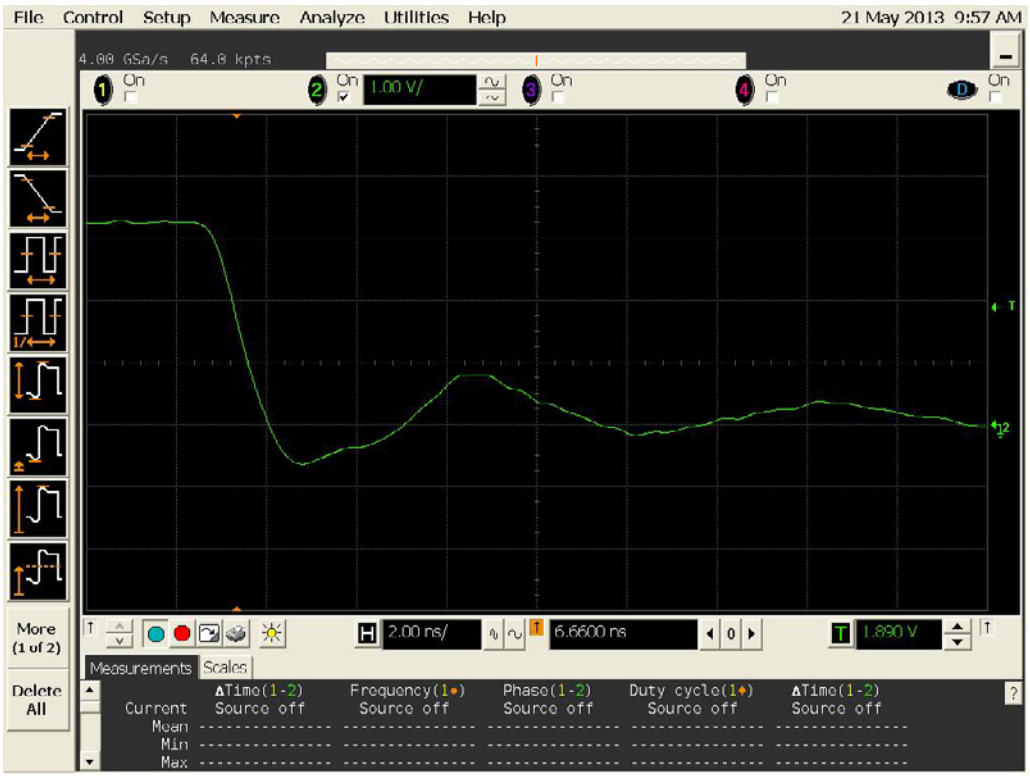

Figure 16b DUT 3411 Post-Annealing Falling Edge.

Figure 17a DUT 3413 Pre-Irradiation Falling Edge.

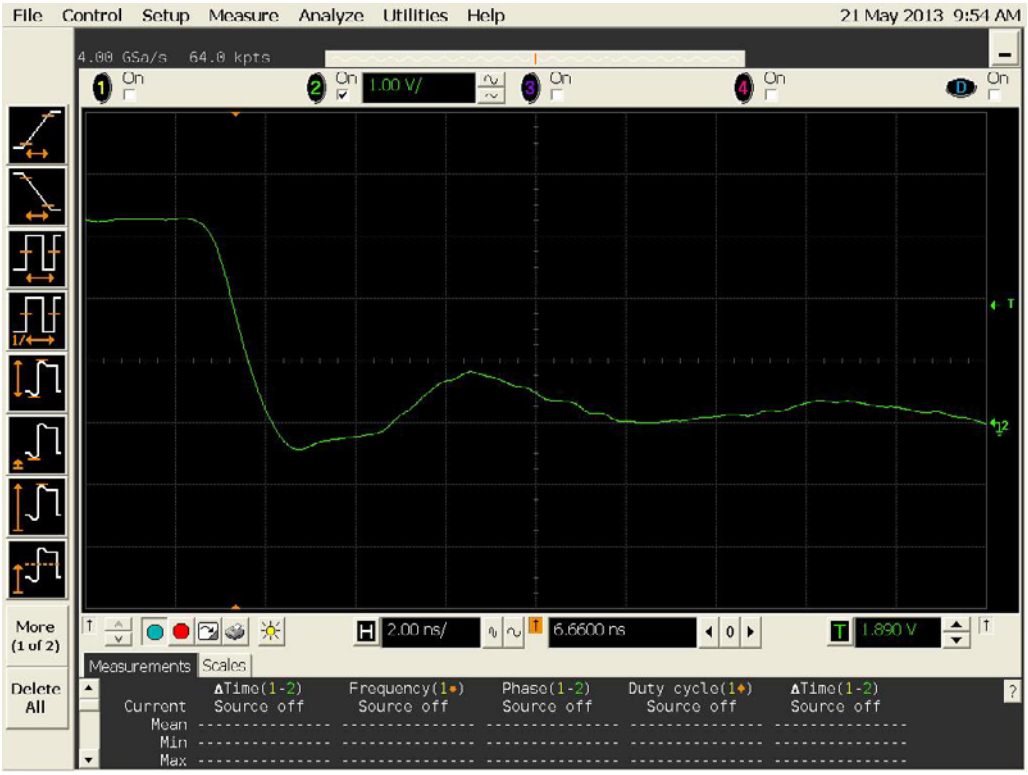

Figure 17b DUT 3413 Post-Annealing Falling Edge.

Figure 18a DUT 3421 Pre-Irradiation Falling Edge.

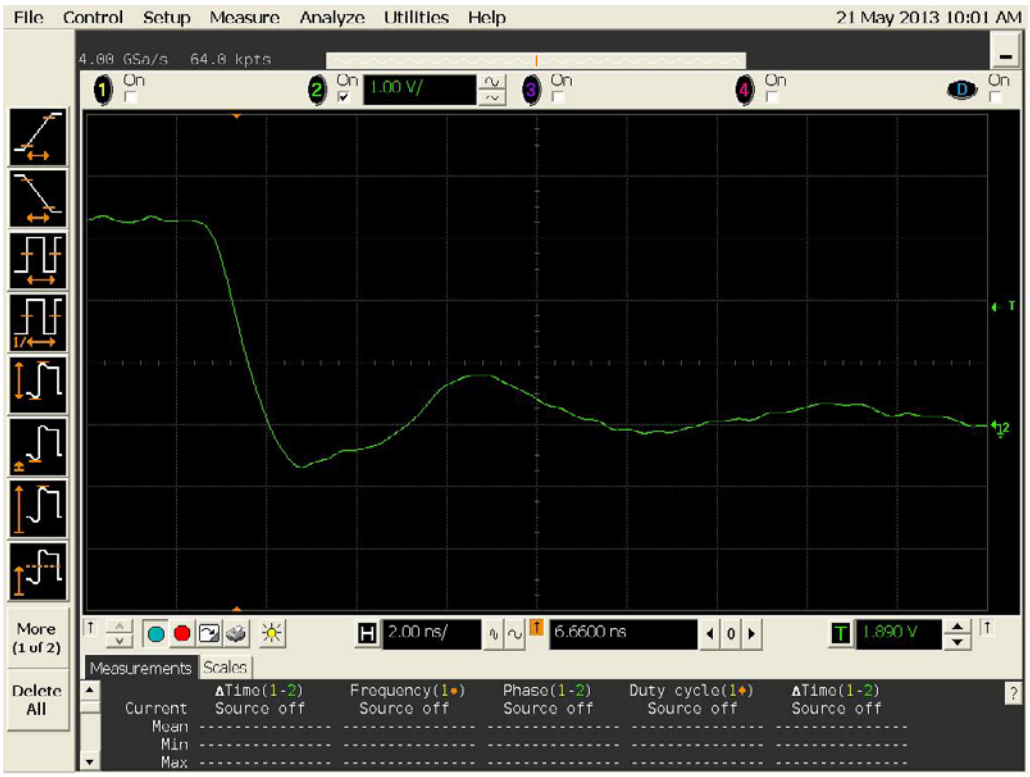

Figure 18b DUT 3421 Post-Annealing Falling Edge.

Figure 19a DUT 3429 Pre-Irradiation Falling Edge.

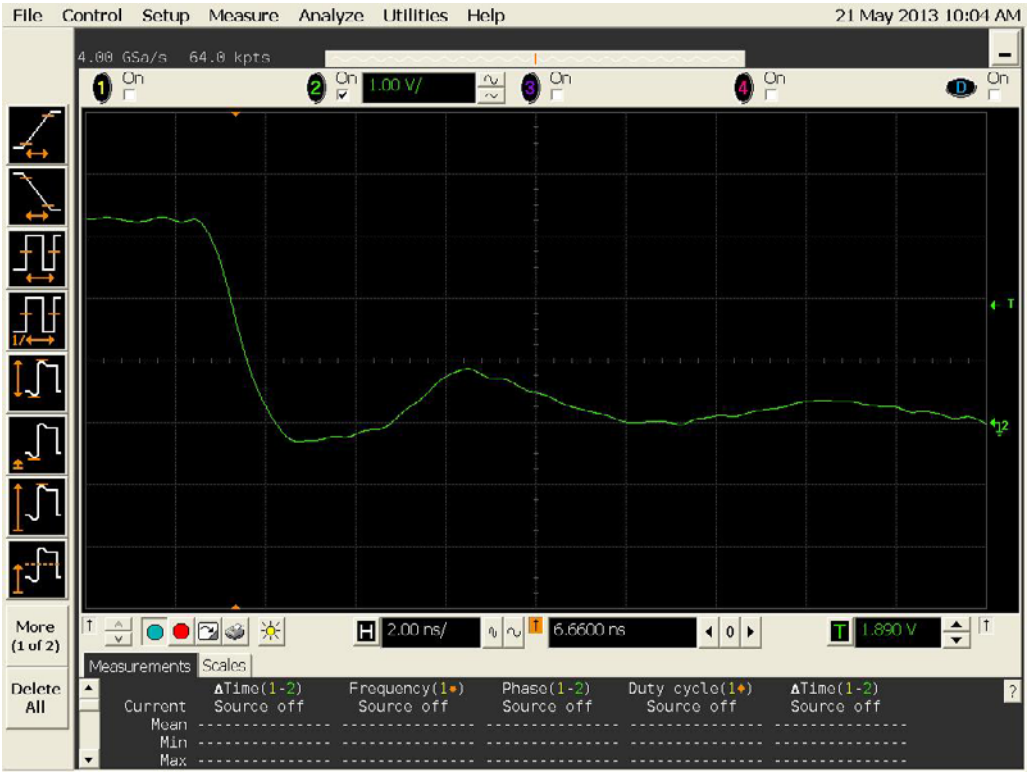

Figure 19b DUT 3429 Post-Annealing Falling Edge.

Appendix A: DUT Bias Diagram

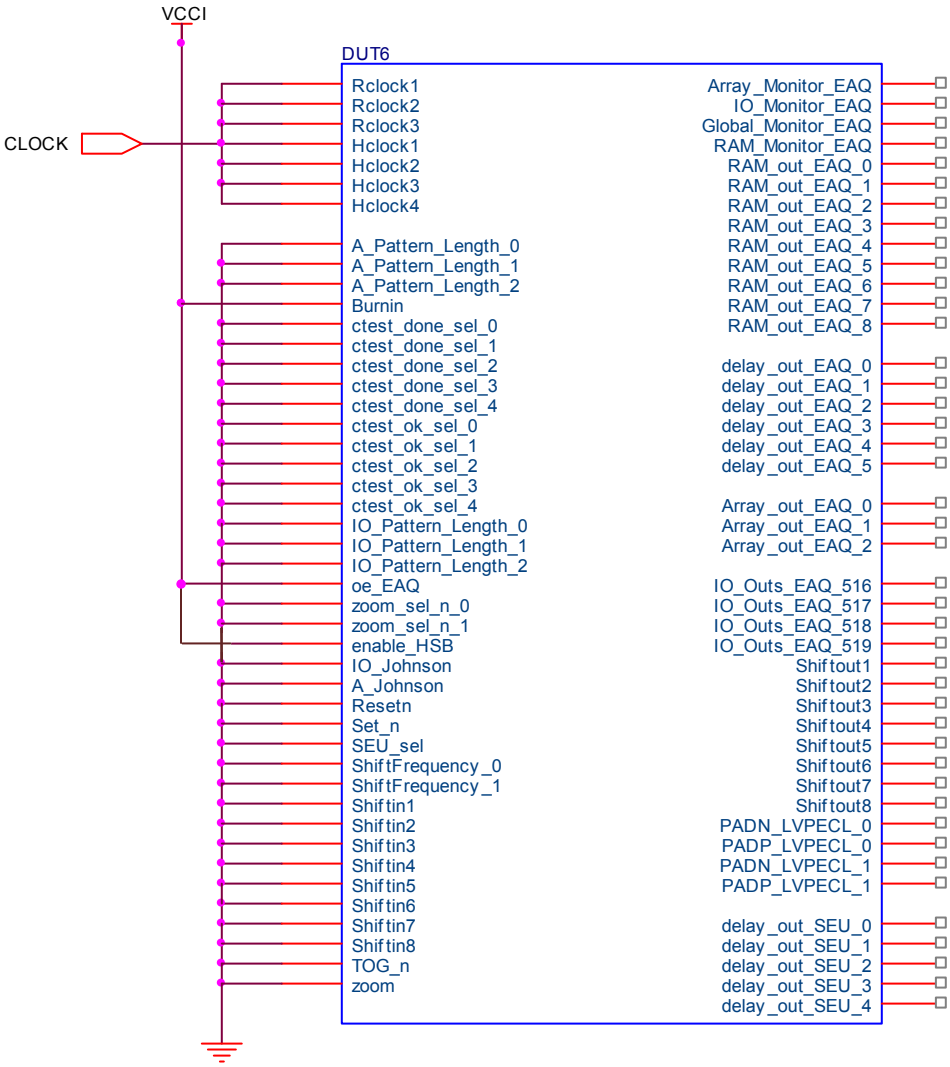

Figure A1 I/O Bias During Irradiation

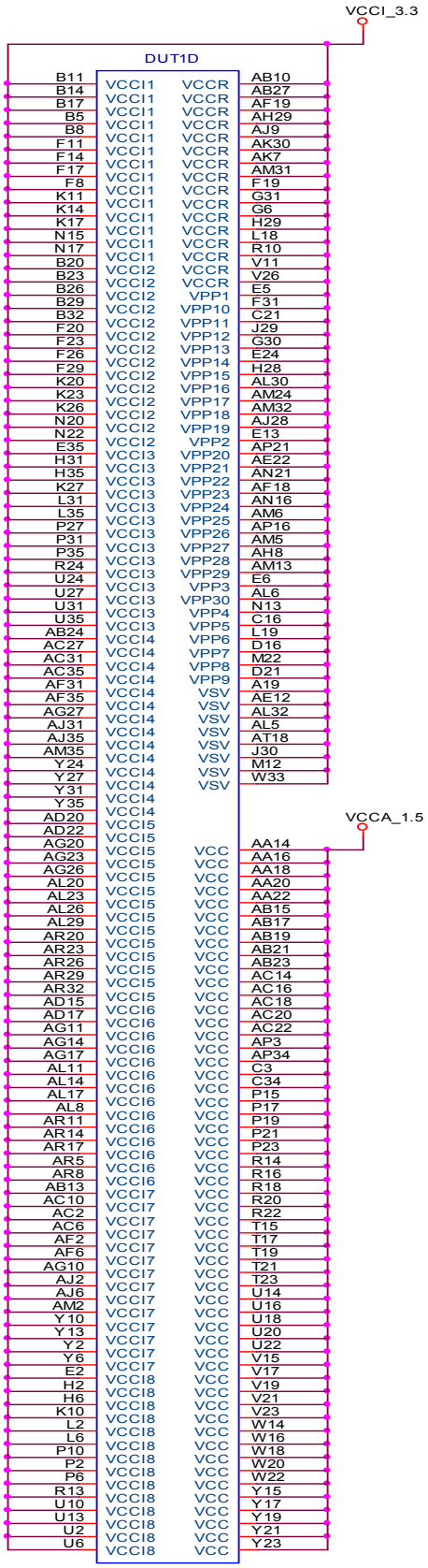

Figure A2 Power supply, Ground and Special Pins Bias During Irradiation

Appendix B: Functionality Tests

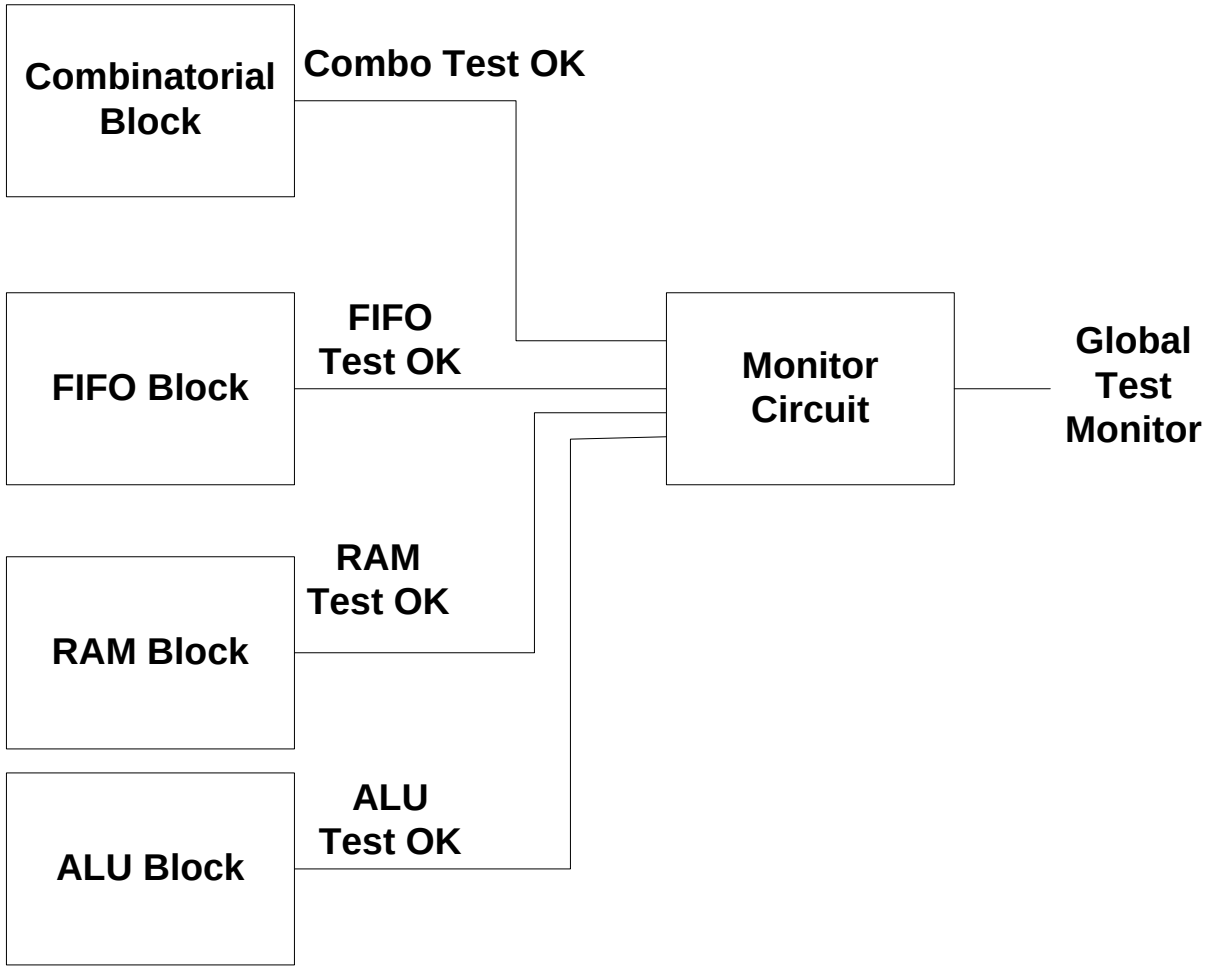

Figure B1 QBI Block – Top-Level Design

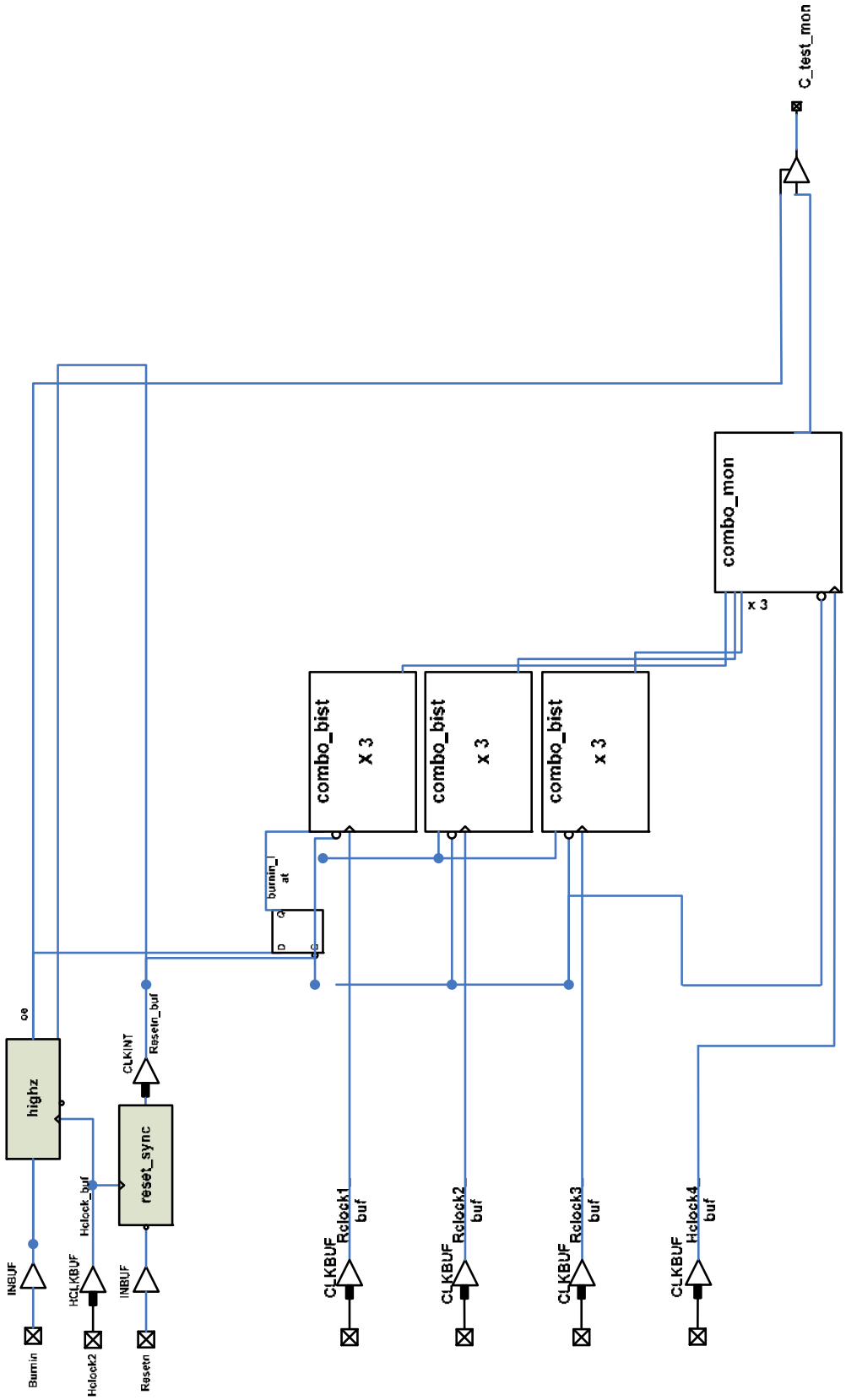

Figure B2 QBI Block – Combinatorial Test (Top Level)

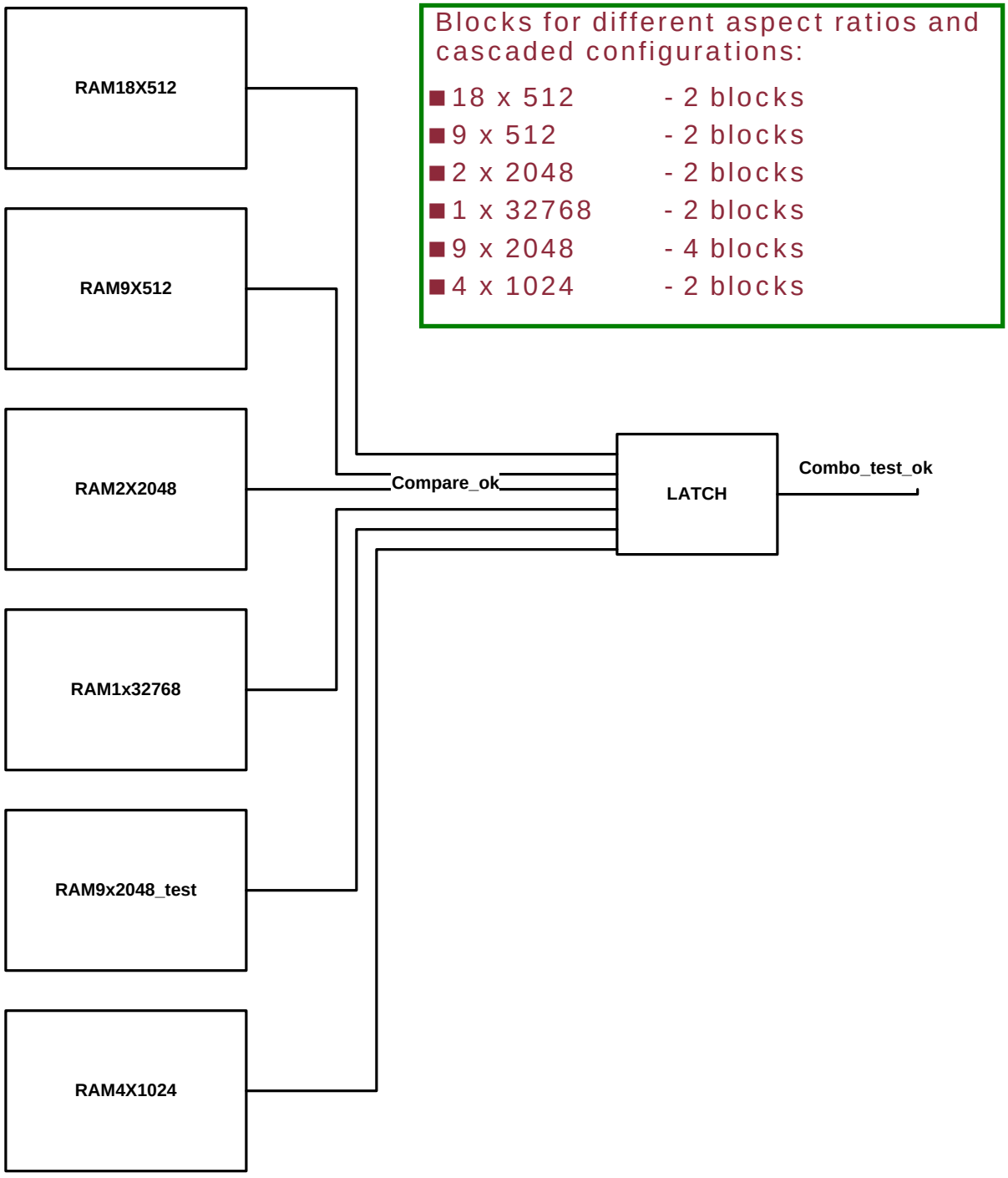

Figure B3 QBI Block – RAM Test (Top Level)

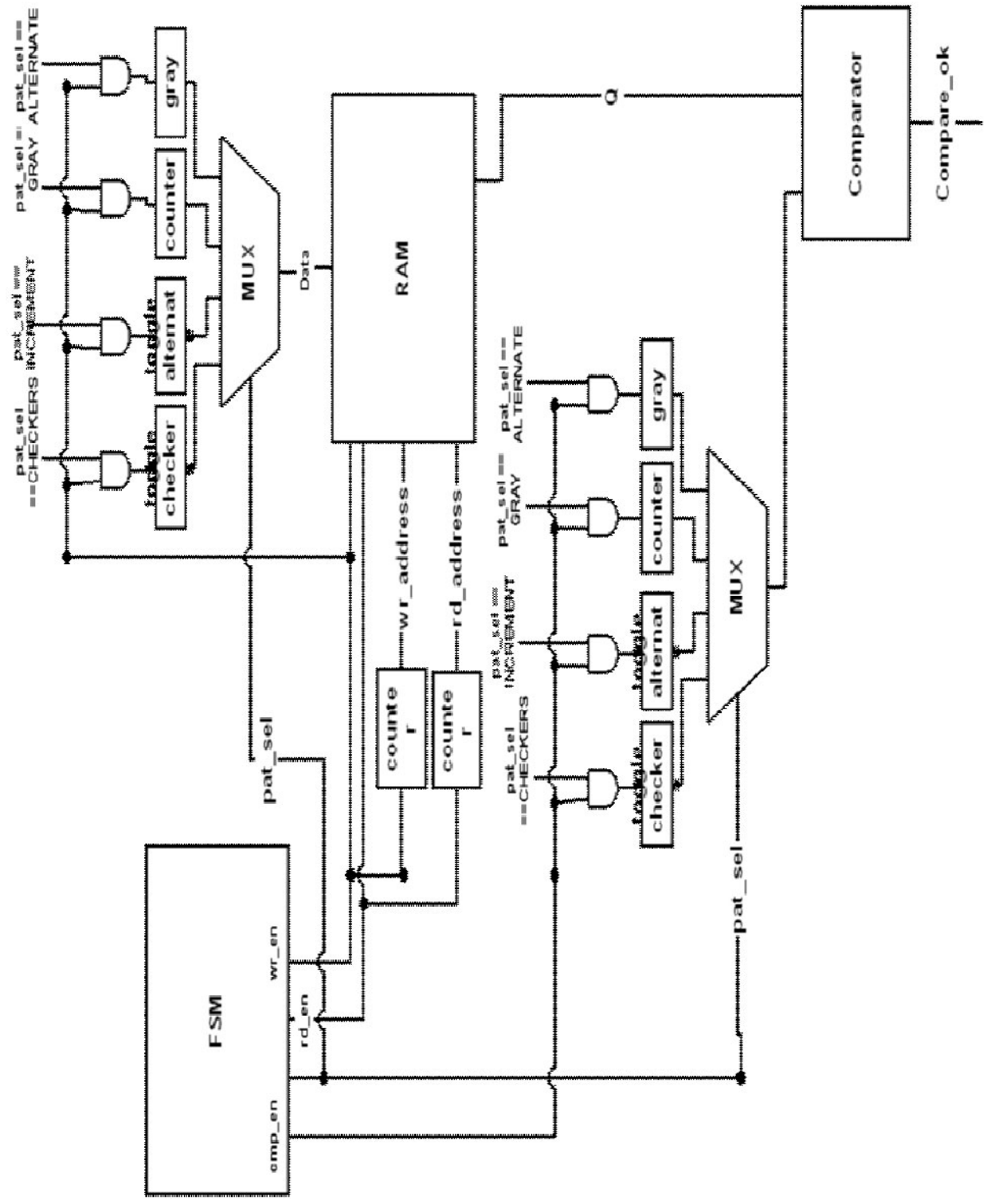

Figure B4 QBI Block – RAM Block

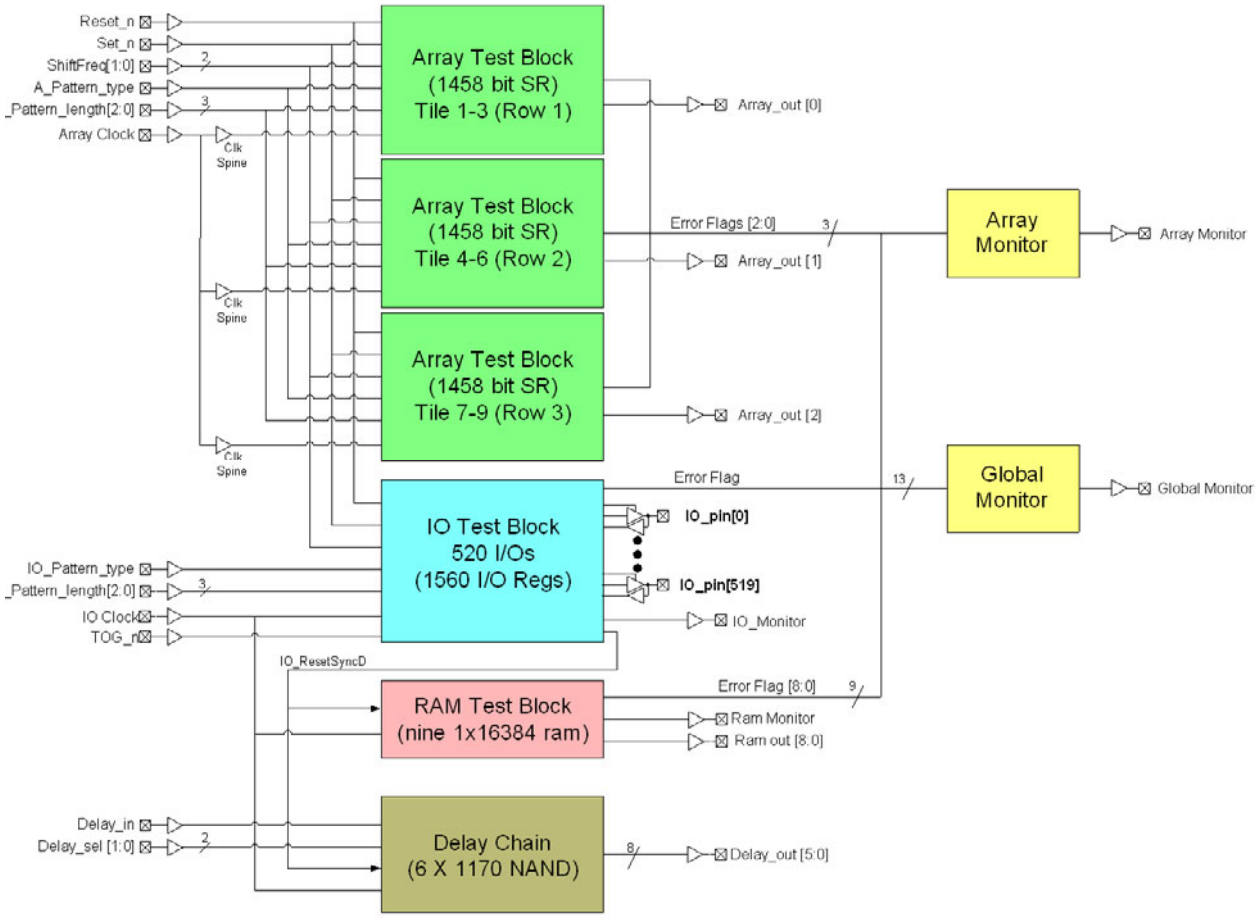

Figure B5 EAQ Block – Top Level

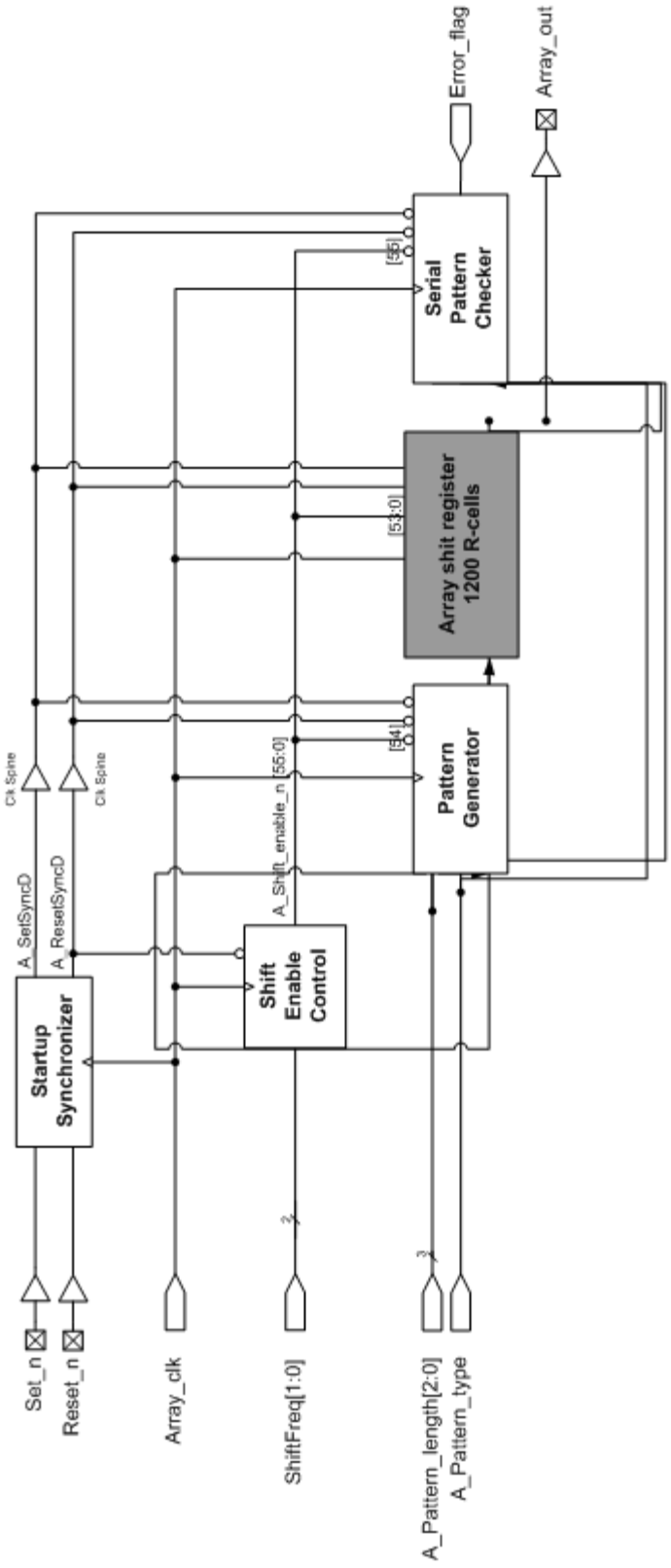

Figure B6 EAQ Block – Array Test (Shift Register)

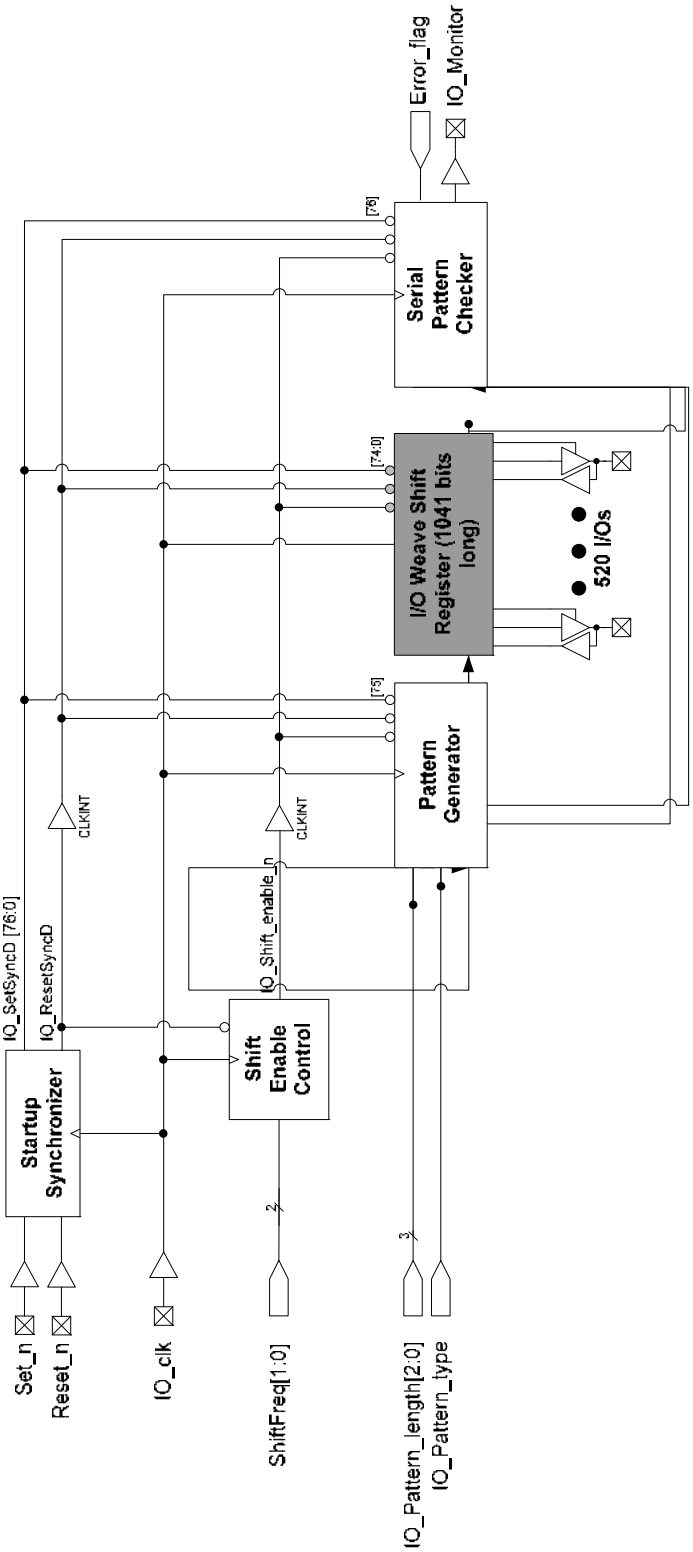

Figure B7 EAQ Block – I/O Test (Top Level)

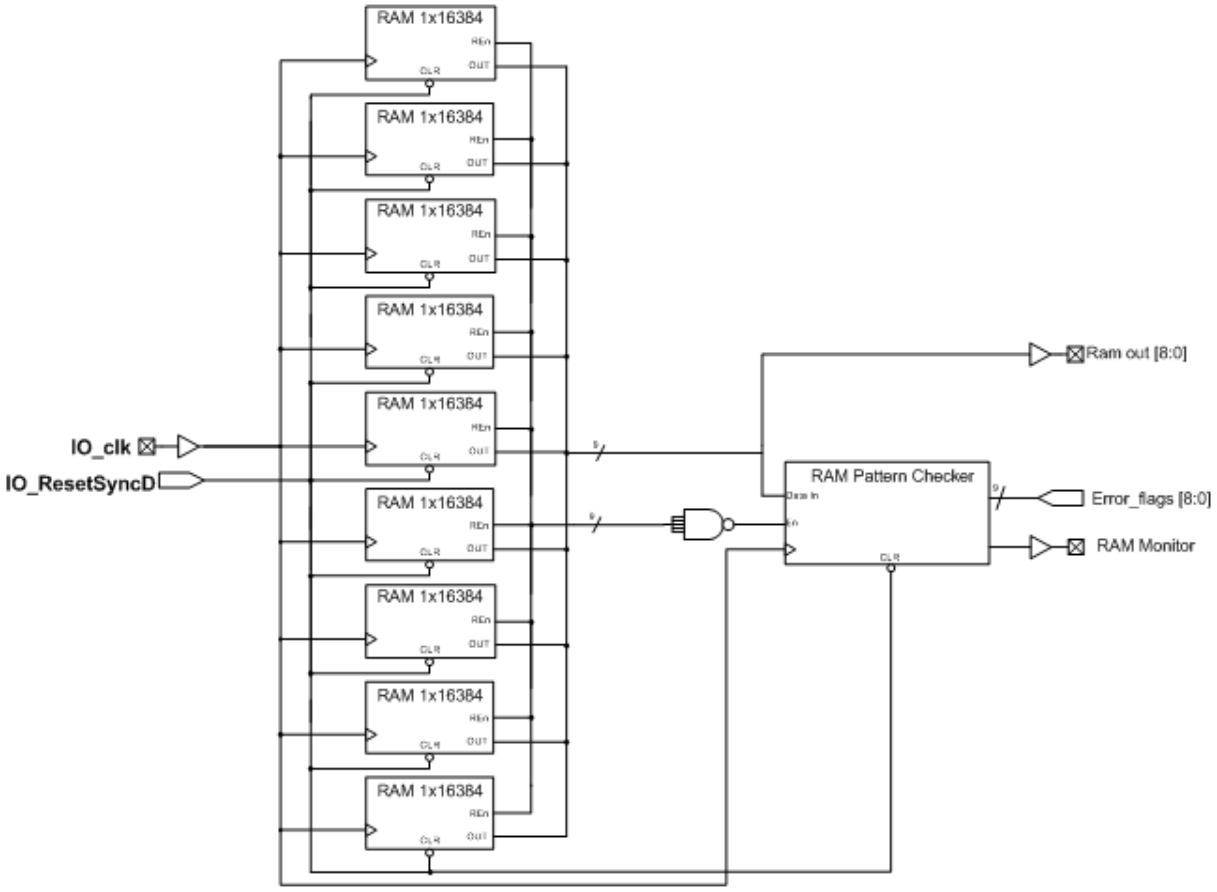

Figure B8 EAQ Block – SRAM Test (Top Level)

Microsemi Corporate Headquarters
One Enterprise, Aliso Viejo CA 92656 USA
Within the USA: +1 (949) 380-6100
Sales: +1 (949) 380-6136
Fax: +1 (949) 215-4996

Microsemi Corporation (NASDAQ: MSCC) offers a comprehensive portfolio of semiconductor solutions for: aerospace, defense and security; enterprise and communications; and industrial and alternative energy markets. Products include high-performance, high-reliability analog and RF devices, mixed signal and RF integrated circuits, customizable SoCs, FPGAs, and complete subsystems. Microsemi is headquartered in Aliso Viejo, Calif. Learn more at **www.microsemi.com**.